



Reconstruction of vegetation during the last 1100 years in northern Central Siberia (Russia) from pollen and geochemical analyses of lake sediments

Diplomarbeit

zur Erlangung des akademischen Grades
Diplom-Geoökologin

vorgelegt von

Liv Heinecke

Universität Potsdam
Institut für Erd- und Umweltwissenschaften

Potsdam, im September 2011



1. Gutachterin: Prof. Dr. Ulrike Herzschuh
Alfred-Wegener-Institut für Polar- und Meeresforschung

Universität Potsdam
Institut für Erd- und Umweltwissenschaften

2. Gutachter: Prof. Dr. Florian Jeltsch
Universität Potsdam
Institut für Biochemie und Biologie

Content

List of Figures	I
List of Tables	III
Abstract	IV
Zusammenfassung	VI
1 Introduction	1
1.1 Scientific Background	1
1.2 Aims and Objectives	2
2 Study Area	3
2.1 Geographic setting.....	3
2.2 Geological and geomorphological setting.....	4
2.3 Soil	7
2.4 Permafrost and thermokarst	8
2.5 Climate	11
2.6 Vegetation	12
3 Methods	16
3.1 Field work	16
3.2 Pollen analyses	17
3.2.1 Pollen sample treatment and pollen analyses	17
3.2.2 Pollen data treatment	18
3.3 Sedimentary analyses	19
3.3.1 Splitting and sample preparation.....	19
3.3.2 Grain size distribution	19
3.3.3 Biogeochemistry: TN, TC and TOC	21
3.3.4 Stable isotope geochemistry ($\delta^{13}\text{C}_{\text{org}}$, $\delta^{15}\text{N}_{\text{total}}$)	22

3.3.5 Hydrochemistry	23
3.4 Age determination	24
4 Results	25
4.1 Field data and results of water ion analysis.....	25
4.2 Results of pollen data and spectra composition	26
4.2.1 General characteristics of the pollen spectra.....	26
4.2.2 Cluster analysis	28
4.2.3 Ordination analysis.....	28
4.2.4 Pollen concentration and influx.....	30
4.3 Results of grain size analyses	31
4.4 Results of biogeochemistry	33
4.5 Results of stable isotope geochemistry ($\delta^{13}\text{C}_{\text{Org}}$, $\delta^{15}\text{N}_{\text{Total}}$).....	34
4.6 Age-depth-model.....	35
5 Discussion.....	38
5.1 Vegetation change during the last 1100 years (From Krasnoyarsk Krai to the entire Arctic).....	38
5.1.1 Pollen source area and productivity reconstruction	38
5.1.2 Vegetation change inferred from pollen data	39
5.1.3 Vegetation response to climate signals and feedbacks.....	41
5.2 Changes in the environmental setting of the north Siberian lake 07-SA-34.....	44
5.3 Limitation of data set and possible enhancements	51
6 Conclusion.....	53
7 References	55
8 Appendix	65
Danksagung.....	68
Selbstständigkeitserklärung	69

List of Figures

Figure 01:	Study area in Northern Central Siberia (globe by Lancer 2008; Satellite picture by Martin Trauth 2011, University of Potsdam; Landsat Image by Frank Günther, 2011). . . 3	3
Figure 02:	Main structure of the Siberian Platform (Koronosky 2002)..... 4	4
Figure 03:	Geographic location of the Popigai impact crater and simplified geology of surrounding area (Vishnevsky and Montanari, 1999). 5	5
Figure 04:	Geological map of the Popigai impact structure (Vishnevsky and Montanari, 1999)..... 6	6
Figure 05:	Soil map of study area and surrounding region (Soil Atlas of the northern Circumpolar Region, European Union, 2010) (star indicates approx. position of lake 07-SA-34)..... 8	8
Figure 06:	Map of Permafrost distribution in the northern circumpolar region; blue – continuous; dark blue – discontinuous; light green – sporadic; dark green – isolated patches; red square indicated study area (from Soil Atlas of the Northern Circumpolar Region, European Union, 2010). 9	9
Figure 07:	Sequence of development of alvar thermokarst relief in central Yakutia, according to Soloviev in French (2007), modified. 10	10
Figure 08:	Climate chart of Khatanga (© 1996-2009 S.Rivas-Martínez, Centro de Investigaciones Fitosociológicas, Madrid)..... 12	12
Figure 09:	Vegetation of Central Siberia (using data from Sochava 1979) (Tishkov, 2002). 13	13
Figure 10:	Latitudinal zonation of the Arctic according to several schemes (modified from Chernov and Matveyeva 1979) (Matveyeva 1994). 14	14
Figure 11:	Latitudinal zonality and floristic provinces of the Russian Arctic (Shahgedanova and Kuznetsov, 2002). 14	14
Figure 12:	A - airborne photo of the vegetation in the regional setting of the lake 07-SA-34; B – Vegetation composition beyond the slope; C - lake and lakeshore vegetation (Photos by U.Herzschuh, S.Müller, 2007.) 15	15
Figure 13:	Preparation and securing of the short core with the UWITEC gravity corer (Photos: U.Herzschuh, S.Müller, 2007). 16	16
Figure 14:	Schematic construction of the laser particle size analyzer with indication of the diffraction angle depending on the particle size (Voigt, 2009). 20	20
Figure 15:	Pollen diagram of the 47 short core samples. Depth and Age (AD; all even ages shown due to legibility) shown on the left hand side. Taxa given in percentages of all terrestrial pollen. Rare taxa (n=15), with an appearance of less than 0.5% in 3 out of 47 samples are excluded from this diagram. Results of the CONISS Analysis are visualised on the right hand side. 27	27
Figure 16:	PCA, displaying the first two axes for the short core 07-SA-34. 30	30

List of Figures

Figure 17:	Pollen concentration and pollen influx diagram for the entire pollen composition, Larix, Betula nana and Alnus and sample Scores of Axis 1 and 2.....	31
Figure 18:	Grain size distribution of short core 07-SA-34, showing the poorly sorted character of the sediment throughout the core.....	32
Figure 19:	Sediment triangle after Shepard (1954) with grain size data of core 07-SA-34.....	32
Figure 20:	Results of grain-size distribution, total nitrogen (TN), total carbon (TC), total organic carbon (TOC), total inorganic carbon (TIC), all given in % as well as the TOC and TN ratio	34
Figure 21:	Isotopic ratios of $\delta^{13}\text{C}$ and $\delta^{15}\text{N}$	35
Figure 22:	Age-depth-model of the upper centimeters, Radiometric chronology of the sediment core 07-SA-34 showing the ^{210}Pb dates and sedimentation rates as well as the approx. 1963 depth suggested by the ^{137}Cs record (report by Appleby and Piliposyan, 2010)...	36
Figure 23:	Age-depth-model; the Pb/Cs dating results as well as the assumed sedimentation rates are shown in red. The ^{14}C dating results with the range of error (1σ range) are shown in blue.	37
Figure 24:	Northern Hemisphere, Arctic, Northern Eurasian and Northern Siberian summer surface-temperature trend over the past 1000 years (MacDonald et al.2008).....	42
Figure 25:	a) Projected position of the treeline in late twenty-first century (according to ACIA 2004), current northern limits of trees (top-Larix; bottom-Picea), Holocene Thermal Maximum northern treeline limits based upon the distribution of radiocarbon dated wood and b) July insolation at 70° and summer sea surface temperatures in the Greenland Sea reconstructed on the base of diatoms (extracts from MacDonald et al.2000 and MacDonald et al.2008).	44
Figure 26:	Elemental and carbon isotopic composition of lake samples. Scheme after Meyers (1994).	47
Figure 27:	Nitrogen and carbon isotopic composition of lake samples.....	50

List of Tables

Table 1: Soil classes present in the study area and surrounding region, according to WRB 2006 (World Reference Base for Soil Resources) (Data from Soil Atlas of the northern Circumpolar Region, JRC European Commission, 2010). 7

Table 2: Permafrost depths and mean annual air temperatures in Russia (Sources: Brown and Péwé(1973), Washburn (1979)) (French, 2007) 9

Table 3: Fine grain size fractions (modified after Scheffer and Schatschabel 2002): 21

Table 4: Hydrochemistry of sampled surface water, * marks concentration below the detection limit (data Moritz Kausche, 2008). 25

Table 5: Results of the detrended correspondence analysis (DCA) performed on pollen data (n=47) from lake 07-SA-34. 29

Table 6: Results of the principal component analysis (PCA). 29

Abstract

The northern Central Siberian Arctic provides many suitable archives for climate reconstructions and presents a highly sensitive eco-region with scarce human disturbance.

The objective of this study was to identify and interpret changes in the vegetation cover during the last 1100 year, by means of a short core, which was cored in 2007 from a lake in the catchment of the Popigai river, Northern Siberia. In order to achieve reliable results, a multi-proxy approach was used to identify alterations in the lake system and its vicinity.

In this study a pollen record was generated and analyzed with statistical means. Further measurements include sedimentary parameters, namely grain size, biogeochemistry (TN, TC, TOC) and stable isotopes ($\delta^{13}\text{C}$ and $\delta^{15}\text{N}$).

The results of the statistical analyses were used to divide the pollen record into five zones. Each pollen assemblage zone (PAZ) is showing a rather specific pollen composition and is indicating changes in the vegetation cover in the lake's vicinity. The relationships among samples and species were investigated using a principal component analysis, revealing a clear treeline signal.

The lower part of the core is reflecting the Medieval Warm Period (MWP), reaching from about 900 AD to 1300 AD. The pollen composition comprises of a rather mixed signal, including tree taxa as well as shrub and herb taxa, yet not displaying a pronounced trend. However, internal sedimentological lake signals, e.g. TOC, TN and $\delta^{13}\text{C}$ show a clear decrease during this time. From approx. 1300 AD to 1550 AD a rather unspecific pollen assemblage was reconstructed. Starting around 1550 AD and lasting until the early 18th century, the vegetation signal showed a clear decrease in tree pollen accompanied by a strong increase in shrub pollen, thereby indicating to the Little Ice Age (LIA). This coincides with the results of the TOC and the TN measurements, which display here their lowest values within this study. Another transition zone, which lasts until the 1970s, separates the LIA from the Global Warming period. This recent warming trend is clearly reflected in the pollen composition of the upper samples, where a pronounced increase of tree pollen as well as a decrease in herb pollen becomes apparent. Biogeochemical results match this trend by displaying the highest values throughout the core in the upper samples. The stable isotope ratios are showing more variability, although the $\delta^{15}\text{N}$ ratios are presenting a slightly positive trend.

Since proxies, especially sedimentary ones, can be reflecting different parameters, the multi-proxy approach proved very useful. The combination of biogeochemistry and stable isotope ratios is used to indicate the source of organic matter in the sediment, identifying a clearly

lacustrine dominated signal in this study. Furthermore, it is possible to draw conclusions concerning the bioproductivity in the lake system from the determined parameters.

The findings presented here are indicating that the major climate phases in the last 1100 years are also reflected in the vegetation and sediment signals in the investigated lake. The end of the Medieval Warm Period as well as the Little Ice Age and modern day Global Warming are well distinguishable in the pollen record.

This study queues well into the ongoing research to understand the reaction and feedbacks of the high latitudes in relation to global climate change and can thereby contribute to a higher resolution as well as a better understanding of the Siberian Arctic.

Zusammenfassung

Die nördliche zentralsibirische Arktis verfügt über viele Klimaarchive, welche sich gut für Klimarekonstruktionen eignen. Sie ist eine hochsensible Ökoregion, welche zudem kaum vom Menschen überformt wurde. Das Ziel dieser Diplomarbeit war es, Veränderungen einer lokalen Vegetation innerhalb der letzten 1100 Jahre zu identifizieren und so gegebenenfalls Klimaveränderungen zu erfassen. Die vorliegende Studie beruht auf einem Kurzkern, welcher 2007 aus einem See im Einzugsgebiet des Popigai Flusses in Nordsibirien gezogen wurde.

Um eine ganzheitliche Betrachtungsweise zu ermöglichen, wurde ein Multi-Proxy Ansatz gewählt. Dieser gestattet es besonders effektiv und umfassend Veränderungen im Ökosystem See und seiner Umgebung festzustellen. Für diese Studie wurde als Untersuchungsbasis ein Pollendatensatz generiert und statistisch ausgewertet. Die durchgeführten sedimentologischen Analysen ermöglichen zudem die Bestimmung von Korngrößenzusammensetzung, biogeochemische Kenngrößen wie Gesamtkohlenstoffgehalt (TC), organischer Kohlenstoffgehalt (TOC) und Stickstoffgehalt (TN) und die Ermittlung von stabilen Isotopenverhältnisse.

Es wurde mit Hilfe statistischer Analysen festgestellt, dass sich der Kern in fünf Pollenzonen gliedern lässt. Jede dieser Zonen zeigt eine differenzierte Pollenzusammensetzung, welche auf Vegetationsveränderungen in der Umgebung des Sees hinweist. Die Ergebnisse der durchgeführten Hauptkomponentenanalyse lassen Rückschlüsse auf die Verschiebung der Baumgrenze zu.

Im ältesten Kernabschnitt, welcher den Zeitraum von ca. 900 n.Ch. bis 1300 n.Ch. umfasst, konnte das Mittelalterliche Klimaoptimum nachgewiesen werden. Die Pollenzusammensetzung für diesen Zeitraum weist ein gemischtes Signal aus Baum-, Strauch-Gräser- und Kräuterpollen auf, zeigt dabei aber keinen eindeutigen Trend an. Im Gegensatz dazu belegen die sedimentologischen Untersuchungen der Seesedimente, so zum Beispiel TOC, TN sowohl als auch das $\delta^{13}\text{C}$ Signal einen deutlich negativen Trend. Im folgenden Kernabschnitt vom Anfang des 14. Jh. bis zur Mitte des 16. Jh. war es nicht möglich, ein eindeutiges richtungsweisendes Pollensignal festzustellen; es handelt sich vermutlich um eine Übergangszone. Im dritten Kernabschnitt hingegen ist ab der Mitte des 16. Jh. eine klare Abnahme der Baumtaxa und zeitgleich ein ausgeprägter Anstieg der Strauchtaxa zu verzeichnen. Diese Phase hält bis zum Beginn des 18. Jh. an und kann mit der Kleinen Eiszeit gleichgesetzt werden. Im gleichen Zeitraum erreichen die biogeochemischen Proxys ihre mit Abstand geringsten Werte, was die Annahme von sichtbaren Auswirkungen der Kleinen Eiszeit weiter unterstützt. Eine abermalige Übergangsphase schließt sich an und im jüngsten

Kernabschnitt ab ca. 1970 zeichnet sich die Globale Erwärmung in den Ergebnissen dieser Studie deutlich ab. Der bis heute anhaltende Erwärmungstrend zeigt sich eindeutig in der Pollentaxazusammensetzung der Proben des letzten Kernabschnittes, in welchen es zu einem rapiden Anstieg von Baumpollen und einem Rückgang von Strauch-, Gräser- und Kräuterpollen kommt. Die biogeochemischen Messungen zeigen ihre höchsten Werte innerhalb des Kernes in den oberen Proben und unterstützen damit die Annahme, dass die moderne Klimaerwärmung im Sediment reflektiert wird. Obwohl die Resultate der stabilen Isotope ein ungenaueres Signal wiedergeben, zeigen die $\delta^{15}\text{N}$ Analyseergebnisse einen positiven Trend.

Da insbesondere sedimentologische Proxys für verschiedene Parameter genutzt werden können, erwies sich der bei den Untersuchungen verwendete Multi-Proxy Ansatz als besonders sinnvoll: Biogeochemische Daten und stabile Isotopenmessergebnisse wurden zum Beispiel genutzt, um Aussagen über die im Sediment enthaltene organische Substanz zu treffen und deren Hauptursprung zu identifizieren. In dieser Studie zeigte sich ein eindeutig limnisch geprägtes Signal, welches Rückschlüsse auf einen geringen Eintrag terrestrischen Pflanzenmaterials zulässt. Darüber hinaus ist es möglich, aus den bestimmten sedimentologischen Parametern Schlussfolgerungen über Veränderungen der Bioproduktivität innerhalb des Sees zu ziehen.

Sowohl die Untersuchung der Vegetationszusammensetzung als auch die Ergebnisse der sedimentologischen Analysen belegen die spätholozänen Klimaschwankungen der letzten 1100 Jahren in der untersuchten Region. Insbesondere das Ende des Mittelalterlichen Klimaoptimums, die Kleine Eiszeit als auch die Moderne Klimaerwärmung sind in dem hier erstellten Pollendatensatz deutlich erkennbar.

Die vorliegende Arbeit ergänzt sehr gut die aktuellen wissenschaftlichen Forschungen, welche sich mit den Reaktionen und Rückkopplungen der Vegetation in Relation zum modernen Klimawandel in den hohen Breiten auseinandersetzt. Sie erhöht die Auflösung der wissenschaftlichen Studien in dieser Region und trägt zum spezifizierten Verständnis der Klimaentwicklung der Sibirischen Arktis bei.

1 Introduction

1.1 Scientific Background

Nowadays the term climate change has become more and more present and politicians and decision-makers need to acknowledge the research findings of scientists and believe in their predictions. Yet in order to attempt to create models and predict future developments, it is necessary to understand the past. Therefore studies are needed which help to understand when thresholds are crossed and how the concerned ecosystems react to changes in their environmental surroundings.

The Arctic, a highly permafrost influenced region, is known to be one of the most sensitive ecosystems on earth, maintaining a most sensitive balance (ACIA, 2004). In the context of global climate change a high risk for the northern regions, e.g. northern Central Siberia, must be assumed.

Global warming might not only lead to higher ice- and snowmelt rates in the high Arctic, which solely would affect the sea-level on a global scale, but also to changes in biome displacements that will be resulting from rising temperatures. Changes in vegetation composition, and especially a northward moving treeline are likely to trigger a positive feedback between climate and vegetation, leading to an even higher rise in temperature, due to a decreasing albedo and increasing solar heating of land (Bonan, 2008). It is expected, that temperatures in high latitudes will exceed the mean global temperature rise by approx. a factor of two (IPPC, 2007). For the Lena delta, a neighboring region of the study area with a similar setting, a mean annual temperature rise of about 0.065 K/a is predicted (Langer, 2006). The general warming trend influences especially the thawing of the active layer, which consequently unfreezes progressively, and is thereby changing parameters in this sensitive system. Higher ground temperatures, thawing of permafrost and enhanced thermal erosion are just a few expected consequences (ACIA, 2004).

Various studies have been done to evaluate the problems occurring in the context of past global warming phases, but these concentrate in most cases on one proxy or on one field of possible methods, e.g. Meyers (1997, 2003) is studying lacustrine organic geochemistry in detail, Andreev and Klimanov (2000) are using pollen records and MacDonald et al. (2000) are focusing on macrofossil dating to reconstruct the treeline movements. In order to get an integrated approach some studies combine proxies from different fields, e.g. MacDonald et al.

(1993) were using pollen and diatoms records as well as sedimental geochemistry to explain the rapid response of treeline vegetation and lakes to past climate warming. Another study by Laing et al. (1999) is investigating past former environmental and climatic changes related to treeline shifts inferred from fossil diatoms and alkalinity. These studies show that a multi-proxy approach can help to evaluate changes concerning the climate and the environment surrounding of the study site.

For these reasons, this thesis was conducted as a multi-proxy study combining pollen analysis, sedimentology and isotope geochemistry. The study site is located in the high latitudes of Central Siberia, a remote and scarcely investigated region, where the Alfred-Wegener Institute of Polar and Marine Research, Potsdam is working in order to acquire knowledge about the development of the Arctic in former times.

1.2 Aims and Objectives

The aim of this study is to reconstruct the vegetation changes and alterations within the lake system during the last 1100 years. In this context the following aims and objectives were formulated:

- Characterization of changes in the vegetation composition
 - by determination of pollen spectra composition
 - by statistical analyses and interpretation of pollen spectra composition with regard to temperature changes
- Reconstruction of changes in the lacustrine system
 - by sedimentary analysis (grain size, biogeochemistry and stable isotopes) conducted on a short core
 - by interpretation of the sedimentary results and already existing surface water analysis concerning alterations in the environmental setting of the lake and changes in temperature
- Comparison of findings - reconstructed from changes in the vegetation composition as well as changes in the lake sediment consistency

2 Study Area

2.1 Geographic setting

The study area is located in the catchment of the Popigai river in northern Central Siberia. The region belongs to the Krasnoyarsk Krai ('territory'), Russia (Figure 01:) and is set in the furthestmost northeast. Krasnoyarsk Krai is the second largest territory, preceded by its eastern neighbour, the Sakha Republic ('Yakutia') and arose from the autonomous Okrug ('district') Taymyr and Evenk. The former Taymyr district is considered the northernmost in the Russian mainland and extends over an area of 862,200km², which is inhabited by approx. 40,000 people, half of which live in the former administrative center Dundinka.

With a population density of only 0.05 inhabitant/km² and most settlements in the vicinity of the major river Yenissei or in the southern part of the district, human influence in the study area is limited.

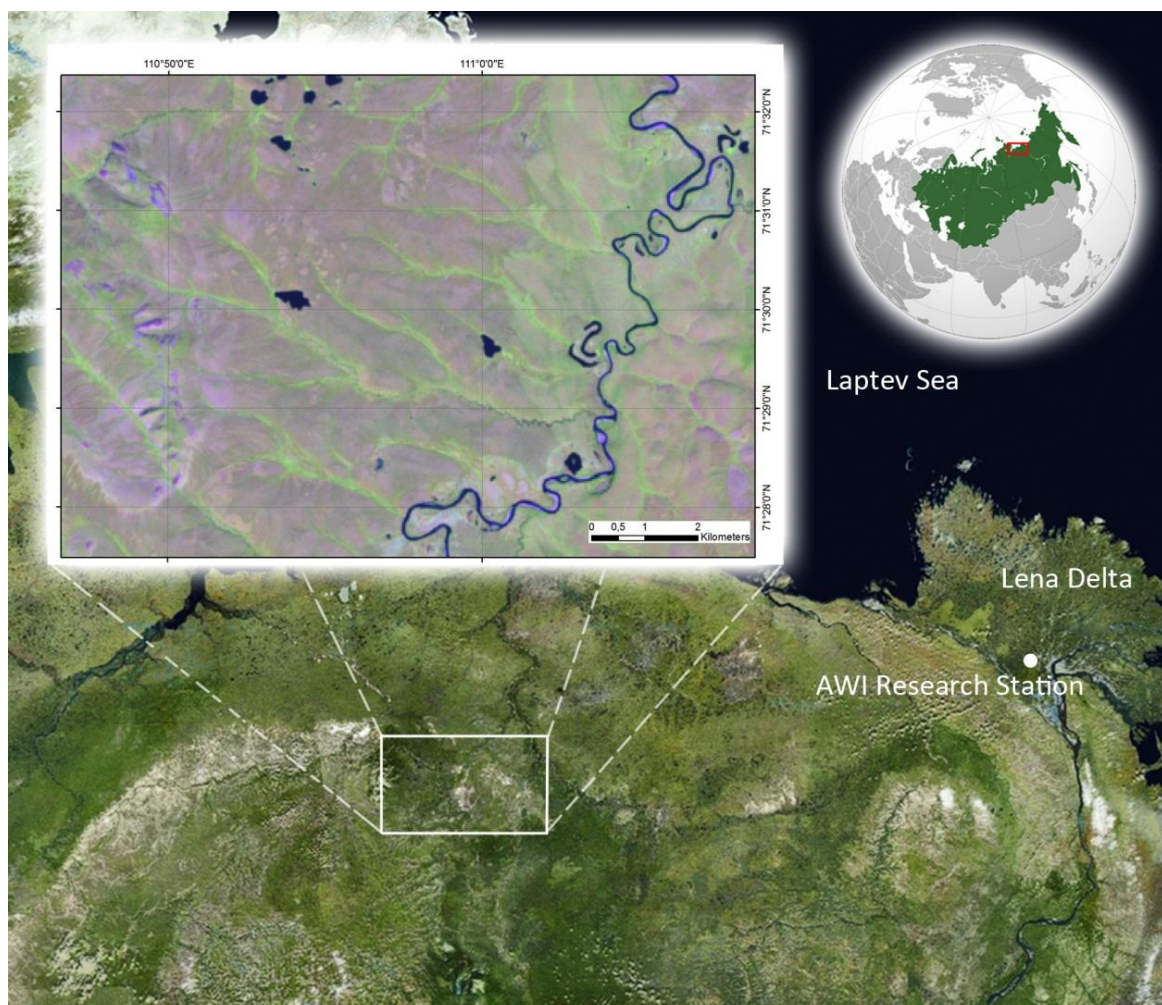


Figure 01: Study area in Northern Central Siberia (globe by Lancer 2008; Satellite picture by Martin Trauth 2011, University of Potsdam; Landsat Image by Frank Günther, 2011).

2.2 Geological and geomorphological setting

The investigated lake 07-SA-34 (71°30'05" N and 110°54'00" E) is located on the Siberian Platform, which stretches from the Yenisey River in the west to the Lena River in the east. It reaches from the Laptev Sea (Arctic Ocean) in the high northern latitudes to the Baikal lake in the South. The Siberian Platform (Figure 02:) basically composes of two levels.



Figure 02: Main structure of the Siberian Platform (Koronosky 2002).

The basement originated from the Precambrian platform and consists of various tectonic blocks, that form the bedrock for the covering Paleozoic deposits (Koronovsky, 2002; Mitrofanov and Taskin, 1994). As most of the sequences originate in the much metamorphosed basement rocks and are heavily granitized, their origin is hard to differentiate (Mitrofanov and Taskin, 1994). Deposits only expose a few particular areas, e.g. the Aldan shield or the Anabar massif, where basement sediments emerge. Throughout the Siberian Platform, Quaternary sediments are widely spread and are to be found in various genetic types. While the north-west is dominated by glacial sediment, the areas further south are mainly covered by periglacial and lacustrine-alluvial sediments (Koronovsky, 2002). Loess, as dune sands or in different stages of genesis can also be found in the more southern parts of the Siberian Platform. During the last glacial, which reached its maximum in the area of the Siberian Platform around 17,000 to 18,000 years ago, the study area remained free of ice masses, as glaciation in north-west Siberia was limited to local iceshields and mainly found in high elevations (Svendensen et al, 2004; Saarnisto, 2001).

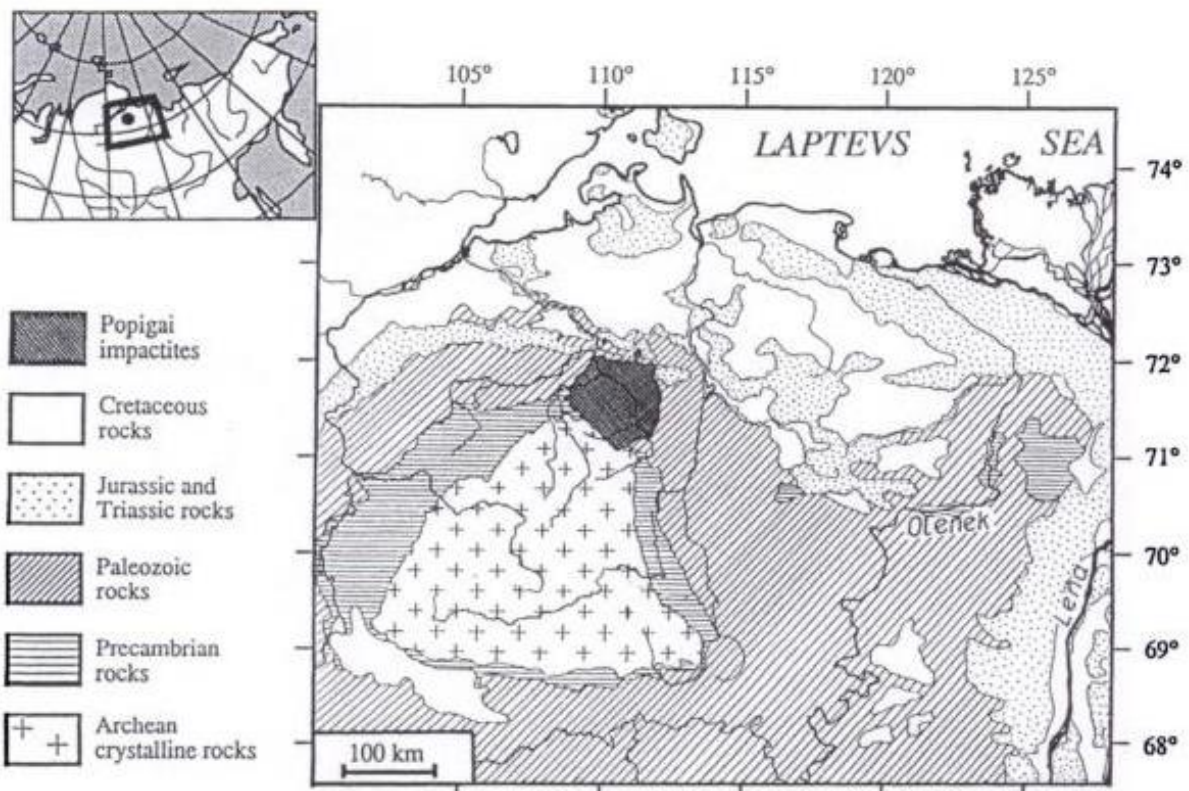


Figure 03: Geographic location of the Popigai impact crater and simplified geology of surrounding area (Vishnevsky and Montanari, 1999).

The lake 07-SA-34 (71°30'05" N and 110°54'00" E) is set in the outer ring of the Popgai Crater (Figure 3) which was first recognized by Masaitis in 1970 (Vishnevsky and Montanari, 1999) and shares the fourth place of impact craters on earth with the Manicouagan Crater (Quebec, Canada). The Popigai crater was formed around 35.7 ± 0.2 Myr. (Bottomley et al. 1997) and is well preserved. The collision with a meteor, 5-8 km in size, created an impact structure of about 100 km in diameter on the northeastern margin of the Anabar shield (Masaitis 2002). Masaitis (2002) states further, that only slightly modified by erosion, the impact site is imprinted as a round-shaped depression with a max. depth of 150-200m (Figure 04) (Pilkington et al, 2002) below the surrounding area. Typical topographic features, such as semi-circular drainage systems, are found as far as 50km from the outer rim crater depression (Masaitis et al 1975).

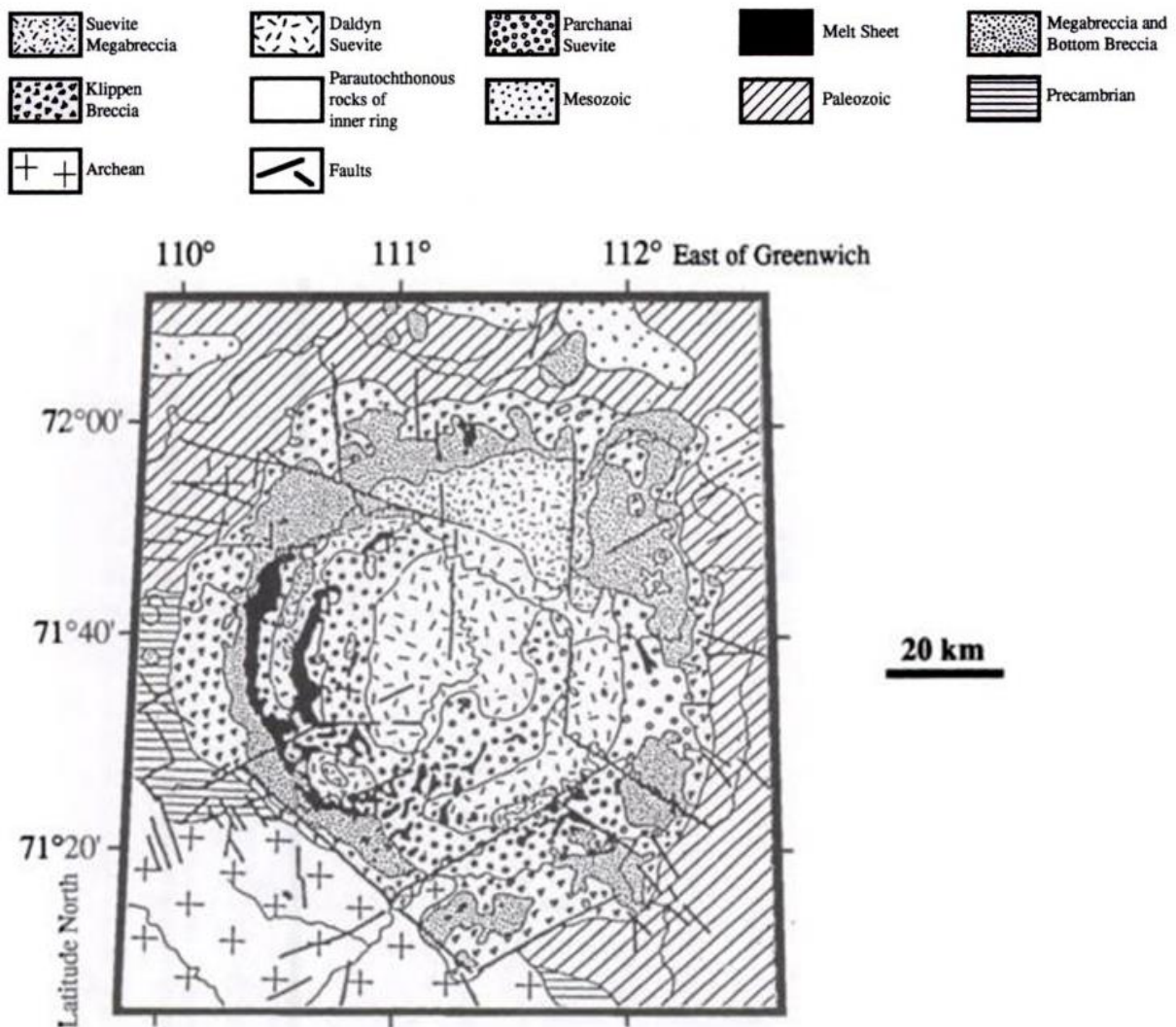


Figure 04: Geological map of the Popigai impact structure (Vishnevsky and Montanari, 1999).

The topography of the study area features a pronounced microrelief comprising of thermokarst lakes, frost heaves, ice segregation, thermal cracking, ice wedge polygons, solifluction and further cryogenic landforms (see chapter 2.3 and 2.4) (IUSS 2007).

2.3 Soil

Soils in the northwest of Siberia are, as are all soils in regions of continuous permafrost (see chapter 2.4), cryosols (IUSS, 2007; Scheffer and Schachtschabel, 2002). Cryosol can be distinguished into four soil groups: cryosol, fluvisol, glysol, leptosol and podsol, which can furthermore be subdivided into several classes (Figure 05). The following classes, displayed in Table 1, were distinguished in the study area and its surrounding.

Table 1: Soil classes presented in the study area and surrounding region, according to WRB 2006 (World Reference Base for Soil Resources) (Data from Soil Atlas of the northern Circumpolar Region, JRC European Commission, 2010).

	Crcc	Calcic Cryosol	permafrost affected soil, accumulation of carbonates
	CRha	Haplic Cryosol	Permafrost affected soil without cryoturbation
Cryosol	CRhi	Histic Cryosol	non-cryoturbated permafrost affected, peaty topsoil
	CRtu	Turbic Cryosol	cryotubated permafrost-affected
	CRum	Umbric Cryosol	non-cryoturbated permafrost affected, acid topsoil
Fluvisol	FLhi	Histic fluvisol	soils in recent river, lake or marine deposits, with a peaty topsoil
Glysol	GLhi	Histic Glysol	peaty topsoil, influenced by shallow groundwater
Leptosol	LPnt	Nudilithic Leptosol	bare rock
	LPrz	Renzic Leptosol	shallow soils over calcareous rock, dark humose topsoil
Podsol	PZet	Entic Podzols	rich in organic matter
	PZrs	Rustic Podzols	acid soil having a pale layer over iron-rich subsoil

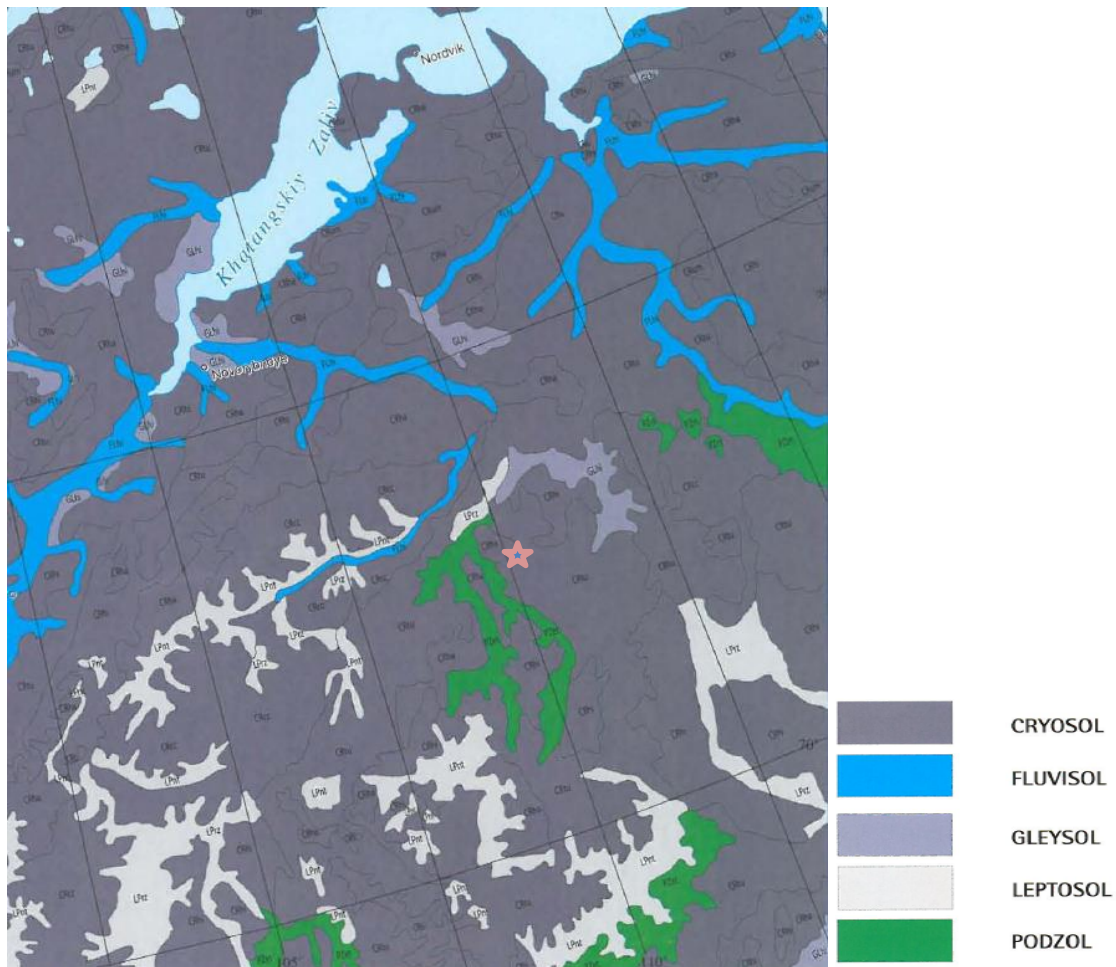


Figure 05: Soil map of study area and surrounding region (Soil Atlas of the northern Circumpolar Region, European Union, 2010) (star indicates approx. position of lake 07-SA-34).

The WRB (ISSU 2007) states, that the parent material can be a “wide variety of material, including glacial till and aeolian, alluvial, colluvial and residual materials”. The dominating soil-forming processes are of cryogenic nature (ISSU 2007).

2.4 Permafrost and thermokarst

Permafrost is defined as “perennially frozen ground which remains at, or below, 0°C for at least two consecutive years” (Jones et al., 2010). Approx. 23-25% of the northern hemisphere is underlain by permafrost (French 2007) and whereas almost all of Siberia is affected by it, about 60% of Russia are swayed by it (Figure 06).

Permafrost can either be occurring continuous (91% - 100% of ground underlain by permafrost), discontinuous (51% - 90%), sporadic (10% - 50%) or as isolated patches (< 10%) (Jones et al. 2010).

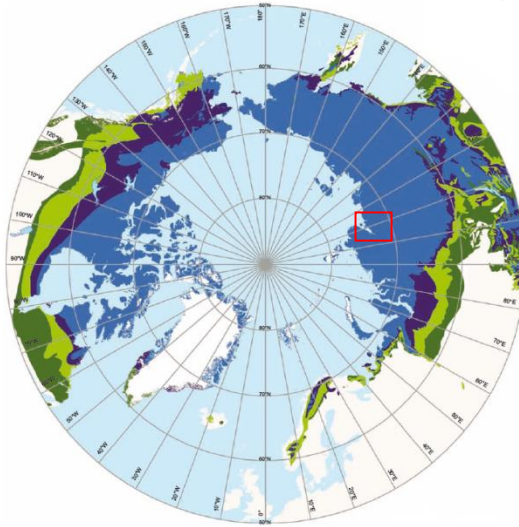


Figure 06: Map of Permafrost distribution in the northern circumpolar region; blue – continuous; dark blue – discontinuous; light green – sporadic; dark green – isolated patches; red square indicated study area (from Soil Atlas of the Northern Circumpolar Region, European Union, 2010).

French (2007) stated that in the northern parts of Siberia, along the Siberian coastal plain, the frozen ground reaches a thickness of up to 600m, decreasing southwards and reaching a maximum depth of about 300m on its southern limits.

Table 2: Permafrost depths and mean annual air temperatures in Russia (Sources: Brown and Péwé(1973), Washburn (1979)) (French, 2007):

	Locality	Latitude	Permafrost Zone	Mean Air	
				Temperature (°C)	Permafrost Thickness (m)
Russia	Nord'vik	72°N	Continuous	-12	610
	Ust'port	69°N	Continuous	-10	455
	Yakutsk	62°N	Continuous	-10	195-250

Permafrost is not only dependent on temperature, but also on further environmental factors, such as relief, rock/soil type, snow cover and vegetation (Washburn, 1980; French, 2007). Whereas vegetation probably presents the most complex and hardest to evaluate, due to its regional and local differences in coverage, cover thickness, isolation value from solar heat etc.. French (2007) points out that several studies indicate that the active layer, the ground that thaws during summer, is most pronounced beneath well-drained bare soil/rock and thinnest

beneath poorly-drained and well-vegetated areas. As a general rule it can be stated, that the active layer is developed thinnest in the Polar Regions and becomes more distinct further southwards.

The main reason for the development of thermokarst depressions is the thawing of ground ice, which can lead to a change in the local or regional geomorphology due to degradation, collapse, subsidence, erosion and instability of the ground surface (Washburn, 1979; Washburn, 1980; French, 2007). The initial formation process might be induced by disturbances of the vegetation cover, fire, the shifting of drainage channels, climate change or by human activity (French 2007).

The typical development stages of Siberian thermokarst lakes are displayed in Figure 07.

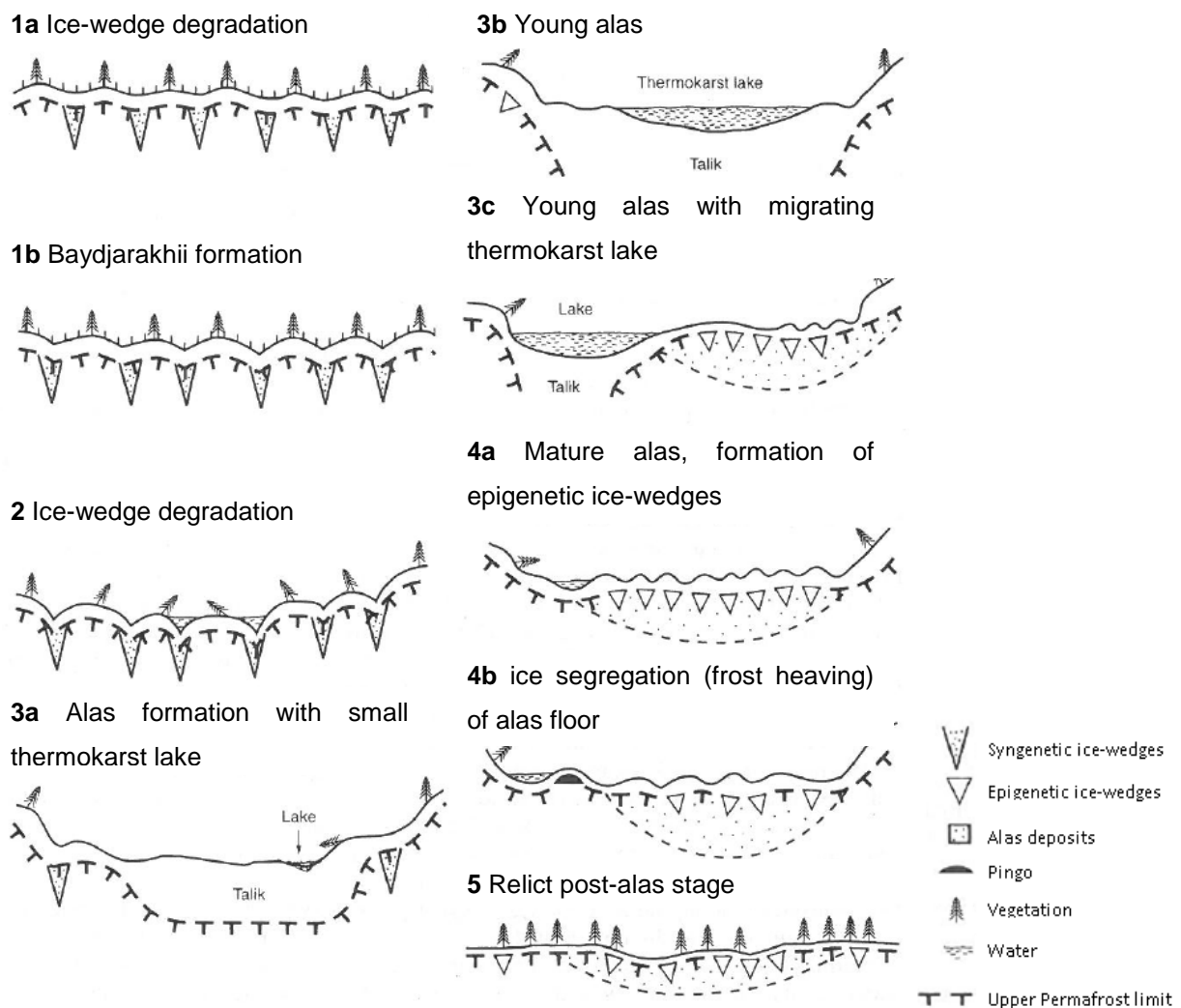


Figure 07: Sequence of development of alas thermokarst relief in central Yakutia, according to Soloviev in French (2007), modified.

2.5 Climate

Northern Siberia is characterized by a high to extremely high degree of continentality (Lydolph, 1977; Przybylak, 2003), because of its location on a huge continental landmass, far away from the Pacific or the Atlantic Ocean, and the northern latitude. As the Arctic Sea remains frozen from October till June, and since pack-ice-covered Sea almost behaves like a landmass from the climatic point of view, the continentality is strengthened (Shahgedanova, 2002).

During the winter months, from November until March, a high pressure system, the so called “Siberian High” builds over northeast Asia and dominates the climatic regime of the region (Przybylak, 2003; Shahgedanova, 2002). In February the winter circulation reaches its high and the Siberian High fades over Siberia and moves westward during April. Around the same time of the year low pressure systems start to develop in the Eastern Siberian area and Far East. During the summer, usually June to September, a low pressure system with low pressure gradients dominates the region, which is replaced by another high pressure system by the beginning of October (Shahgedanova, 2002; Lydolph, 1977, Serreze and Barry, 2005).

In general, there is a temperature gradient from the south-west, more moderate, to the north-east, very cold conditions during winter, due to circulation patterns and also because of the occurrence of polarday (during summer) and polarnight (during winter) north of the polar circle. While the mean annual temperatures are rather low, their annual range is enormous and reaches up to 90-95°C. In winter persistent frosts occur in the study area, whereas up to 30°C (maximum during daytime) can be reached in the summer (Shahgedanova, 2002).

The climate-station close to the study area is located in the village of Chatanga (Figure 08), where the mean January temperature reaches -36.7°C, while the mean July temperature moves up to 17.2°C (1996-2009). Precipitation reaches an average of 331mm per year (in comparison: Berlin 580 mm/a) and falls mainly in the summertime as rain. Whereas August is the wettest month with approx. 50mm, the minimum of about 15mm per month can be found in January, where the precipitation occurs solid due to the low temperatures and forms a thin snow cover. Due to the long winters and the comparatively short summers 40-60% of the overall precipitation falls in solid form.

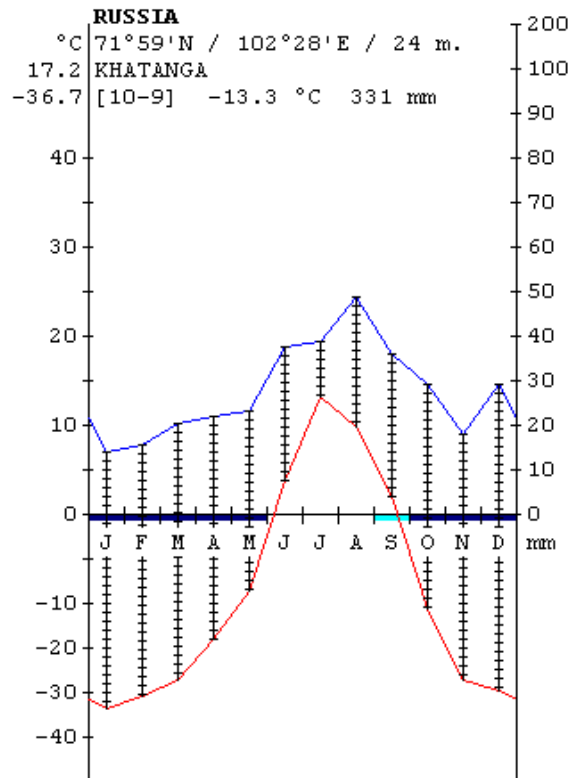


Figure 08: Climate chart of Khatanga (© 1996-2009 S.Rivas-Martínez, Centro de Investigaciones Fitosociológicas, Madrid).

2.6 Vegetation

Vegetation in North Siberia has to cope with one of the most adverse living conditions known on earth. Extremely cold winters in combination with permafrost, low precipitation, a short vegetation period, harsh winds and the pronounced polar night are the main obstacles to overcome. Only cold-resistant species, which are able to reproduce under the given conditions, are able to build long lasting populations.

The general division of vegetation of Central Siberia is shown in Figure 09.

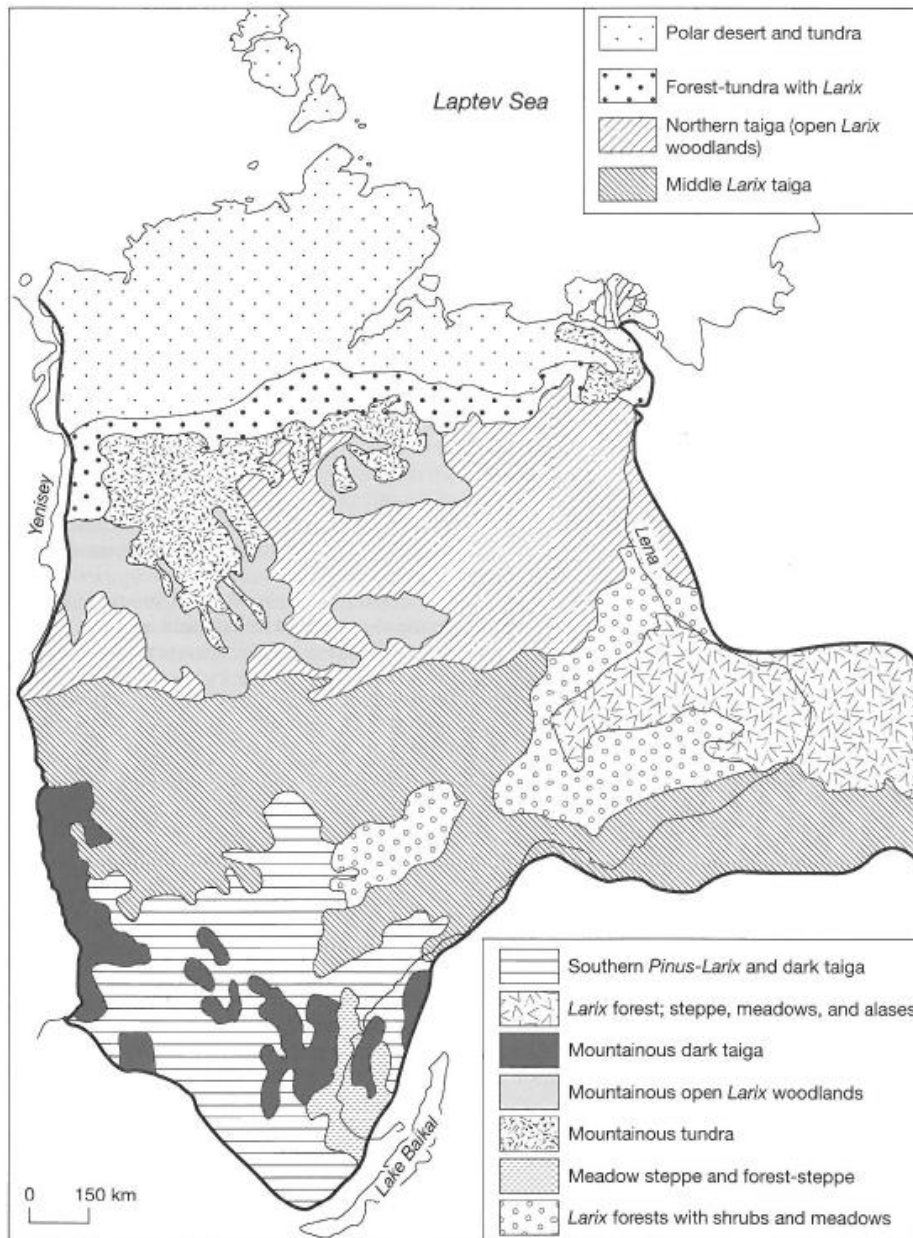


Figure 09: Vegetation of Central Siberia (using data from Sochava 1979) (Tishkov, 2002).

The vegetation that appears in the source area ranges from tundra to forest-tundra. The term ‘tundra’ comes from the Finnish word *tunturi*, which can be translated as “treeless plain”.

Different authors define and divide the tundra into several sub-categories (e.g. Figure 10 and Figure 11). Some count the area surrounding the study area either to the northern ‘typical’ (rarely, in low resolution maps) or the southern tundra on the border to the forest tundra. The northern tundra is defined as covered by “dwarf shrub-herb-moss and dwarf-shrub-lichen” (Resources and Environment World Atlas II, 1998).

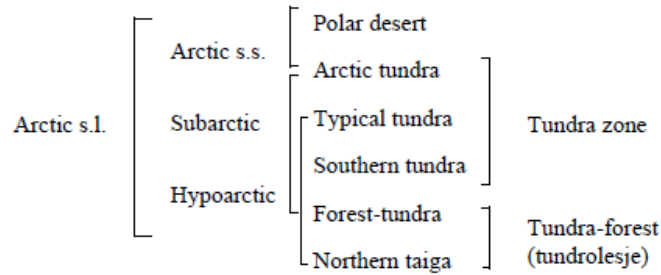


Figure 10: Latitudinal zonation of the Arctic according to several schemes (modified from Chernov and Matveyeva 1979) (Matveyeva 1994).

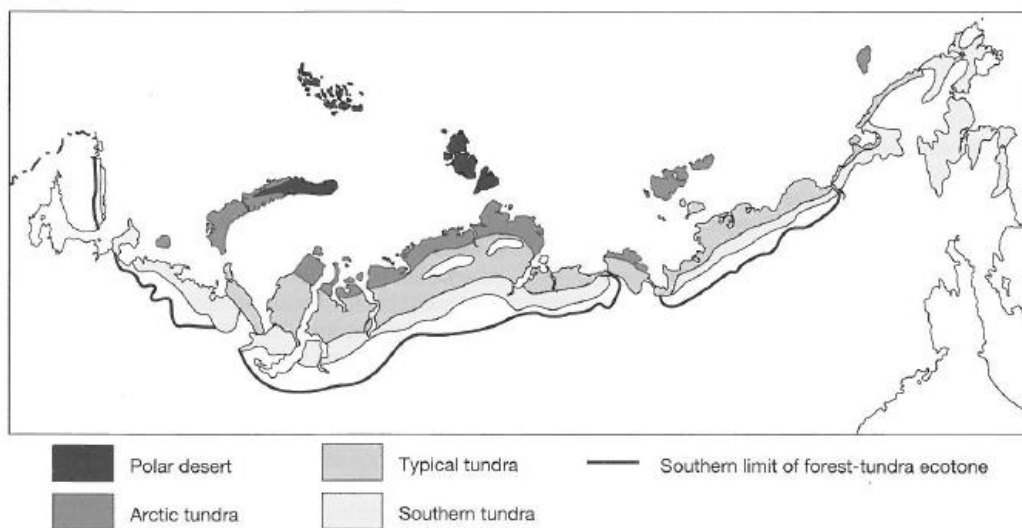


Figure 11: Latitudinal zonality and floristic provinces of the Russian Arctic (Shahgedanova and Kuznetsov, 2002).

The southern tundra is specified as the belt between two sharply differing bioms. In the north the southern tundra is bordered by completely treeless areas, whereas the other side is bounded by forested regions where trees dominate the vegetation (Chernov and Matveyeva, 1997). This ‘transition zone’ lies according to Shahgedanova and Kuznetsov (2002) south of the 8-10°C July isotherm and is characterized as follows: commonly a cover of up to 0.5m high bushes develops on watersheds. Even though there is no tree vegetation, individual trees, mainly *Larix*, often occur in zonal habitats. Patches of woodland develop alongside rivers. *Betula*, *Salix* and *Alnus* are the main components of the shrub layer, although a variety of grass, shrub and dwarf-shrub vegetation can be found in the shelter of trees and bushes. Lichens and mosses cover the entire ground and are speciose.

As the observations during the expedition exhibited, that the studied lake is surrounded by light larix forest, the vegetation at the study site must be counted as forest-tundra.

Generally one might state, that the distribution of vegetation is quite heterogeneous, from small patches of bare ground to distinct herb and shrub layer to groups of bushes and trees all stages can be found, depending on the direct environment. The two driving factors are the local topography as well as the availability of moisture (Shahgedanova and Kuznetsov, 2002). In the direct vicinity of the lake 07-SA-34 a larix cover of up to 30% was determined. The trees grow approx. 5-7m in height. Given that the area framing the lake was very wet, mainly sedges and grass were found on the lakeshore. Above a short slope dryer conditions were found. Here, shrubs such as Ericaceae (*Andromeda*, *Ledum palustre*, *Vaccinium*), *Equisetum*, *Salix* etc. grow in dwarf form, all together accounting for 40% of the vegetation. 90-100% of the ground was overgrown by mosses and lichens (study site data by Dr. Stefanie Müller) (Figure 12). In-the lake underwater *Hippuris* was observed.



Figure 12: A - airborne photo of the vegetation in the regional setting of the lake 07-SA-34; B –Vegetation composition beyond the slope; C - lake and lakeshore vegetation (Photos by U.Herzschuh, S.Müller, 2007.)

3 Methods

3.1 Field work

The helicopter expedition into the Anabar and Popigai region, North Siberia, in 2007 was conducted by Prof. Dr. Ulrike Herzschuh, Alfred-Wegener Institute of Polar and Marine Research, Potsdam, in cooperation with Prof. Dr. Ljudmila Pestryakova, Yakutia State University, Russia. During the expedition the study site of this thesis, lake No. 07-SA-34, was sampled along many others.

The lake was accessed with an inflatable dinghy and spans approximately 300 x 600m. The water depth was ascertained using a hand echolot. A number of limnological parameters were measured on-site, such as conductivity, redox potential, pH and temperature of the surface water (approx. 30cm depth) (WTW Multi 350i). Water transparency was determined by means of a Secchi disc.

In order to obtain well preserved sediment a short core was recovered using an UWITEC gravity corer with a 6cm diameter (Figure 13). The secured short core featured about 33cm of well preserved sediment, which was sliced into 58 samples of approx. 0.57cm thickness in the field to maintain the layer arrangements and prevent any disturbance of the material during transport. The maintained samples were preserved in plastic bags, shut tight and stored cool.

Dr. Stefanie Müller, Free University of Berlin, recorded the vegetation in the lake setting according to the Braun-Blanquet cover-abundance method.



Figure 13: Preparation and securing of the short core with the UWITEC gravity corer (Photos: U.Herzschuh, S.Müller, 2007).

3.2 Pollen analyses

3.2.1 Pollen sample treatment and pollen analyses

A total of 47 pollen samples was prepared and analysed. The preparation of the samples was conducted in the laboratory at the Alfred-Wegener-Institut in Potsdam, where the standard method (Faegri and Iversen 1989) was used to prepare the sample as follows.

During a three day preparation period 1 to 1.5ml of sample material were cleaned and 2 *Lycopodium* spores tablets were added as markers (approx. 10679 spores/tablet; Batch number 938934). On the first day the samples were treated with 10% hydrogen chloride (HCl) to dissolve any carbonate in the samples and to dissolve the substrate of the two added *Lycopodium* spores tablets which consists of calcium carbonate. After the treatment with 10% potassium hydroxid (KOH), including the process of heating the substance in a hot water bath to remove humic acids, the samples were sieved through a 200µm net and after being washed neutral (with a Heraeus Multifuge 1S centrifuge) 40-45% hydrogen fluoride (HF) was added to react with the silicium particles within the samples over night. During the second day, the samples were drained and once more treated with HF, this time supporting the reaction with a hot waterbath and after a heating (1 ½ h), a cooling (1/2 h) and another heating period (1 h) the samples were once more washed neutral and stored over night. Since the remaining water in the samples reacts very strongly with acetic anhydride (C₄H₆O₃), which was added with 96% sulphuric acid (H₂SO₄) for acetolysis in order to colour the pollen grains and spores yellow-brownish, 100% acetic acid (CH₃COOH) was added to remove as much water as possible. After the samples were once more centrifuged neutral, they were sieved through a 7µm net in an ultrasonic bath (VWR USC 100T) to remove all fine material from the samples, which were finally stored in water-free glycerol.

Pollen grains and spores were counted with an Axioskop 40 Microscope (Zeiss) using a 40x objective and 10x ocular and were therefore investigated under a magnification of 400.

At least one slide with a minimum of 300 terrestrial pollen grains, as well as a number of spores and non-pollen palynomorphs (NPP's) was counted for each sample. The NPP's are not included in this thesis since further investigations are necessary for representative analyses.

The pollen grain analysis was based on literature and pollen grain keys of Beug (2004), Chester and Ian (2001) and Moore et al. (1991). Analyses were supported by Dr. Ulrike

Herzschuh and a present day reference collection from Northern Russia, generated by Larissa Savelieva, State University, St.Petersburg.

Most pollen grains are ascertainable on the family or genus level, however *Betula* pollen grains were, because of their distinct appearance, were differentiated into two morphological types: *Betula nana*-type and *Betula alba*-type (Blackmore et al. 2002). The *Betula nana*-type represents the pollen grains of the shrublike growth form and the *Betula alba*-type the treelike growth form of the birch.

3.2.2 Pollen data treatment

A minimum of appearances of each pollen grain type should be assured to include the taxa into further analyses; the threshold in this thesis was set at a minimum appearance of 0.5% in at least three samples out of 47. All pollen taxa and pollen influx diagrams were generated by the TGview software, version 2.0.2. .

In the pollen diagram, taxa were arranged according to their growth form (tree or shrub or herb) and their appearance, as well, in some cases, their taxonomy. All statistical analyses were performed using percentage data.

In order to gain a statistic based cluster analysis, the CONISS software was applied to the pollen diagram. The constrained incremental sum-of-squares cluster analysis was realized on the square-root transformed database to ensure a minimized influence of abundant data (Grimm, 1987). The analysis conducted on stratigraphically sorted samples was carried out to detect differences and similarities over the length of the short core and to structure it into sensible zones.

The usage of analyses such as the cluster analysis as well as a PCA helps to structure the investigated data and reveal patterns. These may to help to find and explain variations or similarities in the pollen spectra composition and help to draw conclusions relating to the scientific research question.

In order to conduct an ordination analysis a detrended correspondence analysis (DCA) and a principal component analysis (PCA) were performed. The aim of these unconstrained ordination methods are to reveal information about the variation in the taxa spectrum, in order to identify the underlying gradients that help explain the data set. As the aim is to reveal information about the cohesion of the pollen taxa within the samples, the species-centred approach was selected (ter Braak and Šmilauer, 2002). All data was square-root transformed to reduce the influence of abundant species and stabilize the variance.

Initially a DCA was performed. The DCA is a modification of the traditional CA (correspondence analysis) to remove the so called “arch” or “horseshoe” configuration in the first two axes of the resulting ordination, which commonly occurs during multivariate methods due to the heterogenic nature of the data (Jackson and Somers, 1991). Depending on the gradient length resulting from the DCA, assumptions concerning the linearity of the data can be made. In case the DCA shows that a linear interpretation of the relationship of the species and the environmental factors is reasonable (if the length of the gradient is <2.5), a PCA can be applied.

The PCA creates a theoretical variable that results in the minimum residual sum of squares. The variable that shows the largest deviance throughout the data set displays the so called first principle component and is indicated by the first axis (ter Braak and Šmilauer, 2002).

DCA and PCA were performed using the software CANOCA 4.5 and biplots were created by CanoDraw for Windows.

Pollen concentration and pollen influx were calculated after Hicks and Hyvärinen (1999).

3.3 Sedimentary analyses

3.3.1 Splitting and sample preparation

The samples for sedimentary analyses were prepared and measured at the laboratory of the Alfred-Wegener-Institut Potsdam, except for stable isotope measurements, which took place at the GeoForschungsZentrum Potsdam (GFZ).

In preparation for the different analyses the original sample was divided into several subsamples, which has to be done with care, as each subsample has to have the same composition as the original sample. Sedimentary analyses were done on all even numbered samples, which lead to a total number of 29 samples for each of the following analyses.

Subsamples that were to be used for geochemical analyses were freeze-dried (Zirbus Sublimator 3-4-5) and subsequently grinded with a Fritsch planetary mill.

3.3.2 Grain size distribution

One of the main soil properties is the structure and the variation of the sediment. To distinguish the structure of the sediment, a laser diffraction particle sizer (Beckmann Coulter LS 200) was used. The principle of laser particle analyses is based on laser diffraction of

particle sizes, the diffraction angle and the light intensities are correlated to a certain grain size. Hereby the laser beam penetrates through filter and projection lenses onto the sample suspension at a right angle and scatters and diffracts on the particles. The generated grain size distinct pattern is focused through a system of Fourier-lenses onto a photodiode detector.

Then, the computer processed the optical data into a digital signal and creates an integral flux pattern of the given suspension with grain sizes ranging from $0.375\mu\text{m}$ to $2000\mu\text{m}$ (HANDBOOK COULTER LS SERIE TEIL III, 1993) (schema see Figure 14).

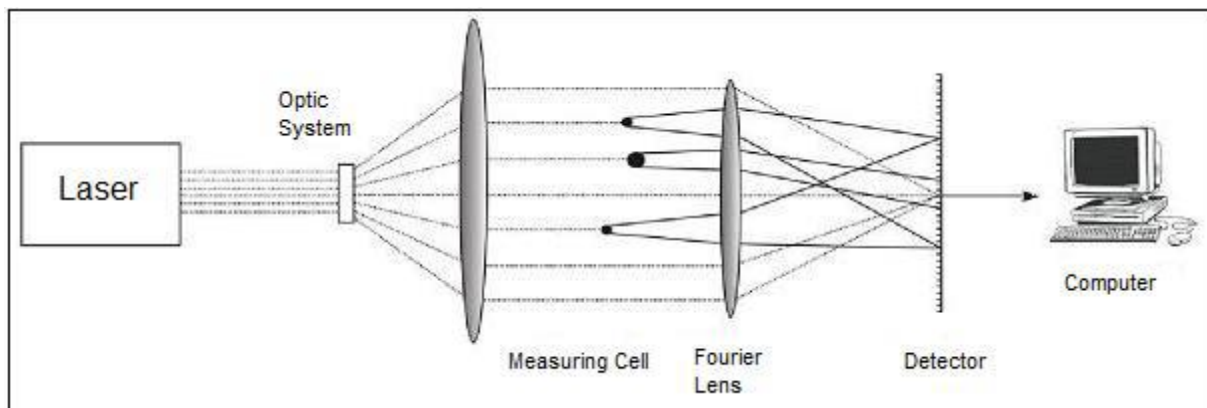


Figure 14: Schematic construction of the laser particle size analyzer with indication of the diffraction angle depending on the particle size (Voigt, 2009).

Since only the clastic components are supposed to be included in the grain size distribution, all organic particles needed to be removed before measurements. This was achieved by placing between 1.92g and 8.99g of sample material on a platform shaker for approx. three to five weeks (Innova 2300) and adding 100ml of a 3% hydrogen peroxide (H_2O_2) solution and two drops of ammoniac for an initial reaction. Afterwards, three times a week 10ml of 35% H_2O_2 were added to the sample until no further reaction could be observed. The carbonates were dissolved using 100ml of 10% acetic acid. After 24h the samples were washed to a neutral pH in a Heraeus Cryofuge 8500i and the sample size was reduced in the Heraeus Multifuge 3s. Subsequently, the samples were dried in a Memmert cabinet drier at 50°C . 0.44-3.54g of organic and carbonate free material were dispersed with approx. 5g sodium pyrophosphate ($\text{Na}_4\text{P}_2\text{O}_7$) and 0.75 l of ammonia solution (0.0001% NH_4) and placed in an overhead shaker (Gerhardt Laboshake) for at least 12h. After the required amount of time each sample was divided into eight homogeneous subsamples by the Rotary sample Divider laborette 27.

Each sample was measured two to five times and the results for further statistical evaluation were averages of these measurements. Grain sizes were classified after Scheffer and Schatschabel 2002 (Table 3).

Table 3: Fine grain size fractions (modified after Scheffer and Schatschabel 2002):

Phi	9	7	6	4	2	1	-1
µm	<2.0	<6.3	<20	<63	<200	<630	<2000
(mm)	(<0.002)	(<0.0063)	(<0.02)	(<0.063)	(<0.2)	(<0.63)	(<2.0)
		fine	middle	coarse	fine	middle	coarse
	Clay		Silt		Sand		

3.3.3 Biogeochemistry: TN, TC and TOC

The organic matter content and composition in the sediment are residues of past biota and therefore a well suited archive, which can provide palaeolimnological information (Meyer, 1997; Meyers and Lallier-Vergès, 1999). As the formation, decay and accumulation of organic substances is considered to be dependent on different environmental factors, such as precipitation, temperature regimes and sedimentary characteristics, the measurement of biogeochemical parameters is used to gain information about the bioproductivity, the decomposition and accumulation of organic matter in the sediment.

The biogeochemical parameters total nitrogen (TN), total carbon (TC) and total organic carbon (TOC) were determined and the TOC/TN ration and total inorganic carbon (TIC) was calculated as follows (Eq. 1 and 2):

$$C/N = TOC/TN \quad \text{Eq. 1}$$

$$TIC = TC - TOC \quad \text{Eq. 2}$$

TOC/TN ratio can be used to identify the mineralisation rate of organic components, as well as, in addition to stable carbon isotope contents (see chapter 3.3.4), may reveal information about the organic content, their biological origin and their degree of decay.

The sediment samples were analysed with the elemental analyser Elementar Vario EL III, which basic principle is based on catalytic tube combustion with oxygen supply at high

temperatures (Handbook Elementar Vario EL III, 2001). The combustion takes place in an oxygen enriched environment at approximately 1150°C. After the removal of foreign gases, Helium (He) serves as a carrier gas and transports the gas mixture through adsorption columns where C, N and S are separated. The percentage of carbon and nitrogen is subsequently calculated in comparison to its input sample weight.

Approx. 8mg of the dried and grinded samples was weighed into tin capsules. Each sample was measured twice and the average was used for further analyses, if the variance of the two measurements was less than 3%, otherwise a repetition was conducted. To detect background noises, blank capsules were determined. Calibration standards were measured in the supposed range of content for each of the determined elements and control standards were analysed every 15 samples to assess the overall deviation of the system and to ensure the precise results with a device-specific accuracy of $\pm 0.1\text{wt}\%$.

TOC measurements underwent the same procedure, but in addition needed to be decarbonized, which was achieved by adding 4% hydrochloric acid (HCl) to the samples and placing them on a heating plate (Störktronic Präzitherm) for three hours at 97°C. Afterwards the carbon free samples were washed neutral by decantation. Spare water was removed by means of vacuum filtration equipment and a drier cabinet (Memmert) and the dry material was homogenised with a pestle.

3.3.4 Stable isotope geochemistry ($\delta^{13}\text{C}_{\text{org}}$, $\delta^{15}\text{N}_{\text{total}}$)

Chemical elements can have different number of neutrons, which means they can appear as different isotopes. Isotopes are generally split into instable and stable isotopes.

Carbon (C) for example has two stable isotopes, ^{12}C and ^{13}C and only one unstable isotope ^{14}C , which is used in dating (see chapter 3.4), whereas nitrogen (N) only occurs in two isotopes, ^{14}N and ^{15}N , which are both stable.

During the metabolism of living plants and during the decomposition after their death, isotopic fractionation takes place within the plant tissue (Degens, 1969). The remains of this tissue are stored in the sediment and by analysing lake deposits, we can therefore draw conclusions about environmental factors such as temperature and the availability of water and nutrients (Meyers and Lallier-Vergès, 1999). The gathered data may also be used to draw conclusions about the productivity rates in former times and to relate the found signal to the metabolism of C_3 , C_4 plants or algae (Meyers and Teranes, 2001).

The $\delta^{13}\text{C}_{\text{org}}$ and $\delta^{15}\text{N}_{\text{total}}$ values were measured by an elemental analyser (NC2500 Carlo Erba) coupled with a ConFlowIII interface on a mass spectrometer (DELTAplusXL) with an analytic precision of $<0.2\%$.

As the organic $\delta^{13}\text{C}$ was to be determined, calcium carbonate free samples (procedure see chapter 3.3.3.) were used. Since the required weighed in material is dependent on the amount of organic carbon stored in the sediment, the encapsulated sample weight (between 3.61-10.22mg) was calculated as follows (Eq. 3):

$$\text{sample [g]} = 20 / \text{TOC} \quad \text{Eq. 3}$$

For $\delta^{15}\text{N}_{\text{total}}$ measurement approx. 20mg of original grinded sample material was weighed into tin capsules and released via auto sampler (AS200) into the elemental analyser. Here, the combustion of the samples took place under the influence of high temperature and added oxygen, thereby producing the sample gas, which was carried by helium into the isotope-ratio mass spectrometer (IRMS). Each sample was measured twice and results were averaged. Blanks and control standards were detected every 10 samples to rule out systemic errors in the measurement.

The findings are given in delta notation to point out the difference between the isotopic ratio of the sample in relation to the international standard (Craig, 1953) (Eq. 4 and 5):

$$\delta (\text{‰}) = [(R_{\text{sample}} - R_{\text{standard}}) / R_{\text{standard}}] \times 1000 \quad \text{Eq. 4}$$

$$\text{with } R = \text{Number of seldom isotope} / \text{number of often isotope} \quad \text{Eq. 5}$$

The standards used for $\delta^{13}\text{C}_{\text{org}}$ are $^{13}\text{C}/^{12}\text{C}$ as well as Vienna PeeDee Belemnite (VPDB) and for $\delta^{15}\text{N}_{\text{total}}$ are $^{15}\text{N}/^{14}\text{N}$ and air.

3.3.5 Hydrochemistry

Hydrochemical analyses of the water surface sample (depth 30cm) have been conducted by Moritz Kausche in the laboratory of the Alfred-Wegener-Institute in Potsdam. Anions were measured using an ion chromatograph (Dionex DX-320), which is a High Performance Liquid Chromatography (HPLC) system. Cations were determined by means of inductively coupled plasma optical emission spectrometry (ICP-OES) (Perkin-Elmer Optima 3000 XL).

3.4 Age determination

Two methods were used to date the short core. In order to get as precise as possible dating results and a good insight into the sedimentation over time, radiometric dating was conducted on the upper 10 samples. This was done by P.G. Appleby and G.T. Piliposyan at the Environmental Radioactivity Research Center at the University of Liverpool, Great Britain.

Dried subsamples were sent in and analysed with regard to ^{210}Pb , ^{226}Ra and ^{137}Cs .

The determination took place by means of Ortec HPGe GWL series well-type coaxial low background intrinsic germanium detectors (Appleby et al. 1986). ^{210}Pb (half-life period 22.3 years) and ^{226}Ra (half-life period 1602 years) were measured via their gamma emission emitted by their daughter radionuclide after three weeks of storage in sealed containers, to allow radioactive equilibration. ^{137}CS was also ascertained by measuring its emissions.

Calibrations were done by determination of samples with a known activity to detect the overall deviation of the detectors used (Appleby and Piliposyan, 2010).

As a second method ^{14}C was used to complement the age determination of the core. In this course 3 subsamples (07-SA-34 05, 07-SA-34 37 and 07-SA-34 56) from a mean sample depth of 2.57cm, 20.81cm and 31.64cm were sent to the Leibniz Laboratory for Age Determination and Isotope Research at the Christian-Albrechts-University in Kiel, Germany, where the samples were checked for contaminations microscopically. The sample material was treated with 1% HCl (hydrogen chloride), 1% NaOH (sodium hydroxid) at 60°C and again with 1% HCl to extract the leaching residue. All fractions were combusted at 900°C to obtain CO_2 , which was reduced with H_2 (hydrogen) to be measured in an accelerator mass spectrometry (AMS). ^{14}C -concentrations were ascertained in accord to the ^{14}C , ^{13}C and ^{12}C content of CO_2 -Standards as well as appropriate background noise detection samples. The conventional ^{14}C -Age was calculated after Stuiver and Polach (Stuiver and Polach, 1977) in connection with an adjustment factor from the isotope-fractionation of, also measured with the AMS, $^{13}\text{C}/^{12}\text{C}$ -ration (Drevers, 2011).

4 Results

4.1 Field data and results of water ion analysis

The lake 07-SA-34 is located in the geological region of the Popigai crater in northern Central Siberia and therefore the relief features a series of smaller elevations in the surroundings. The lake itself is located at 71°30'05" N and 110°54'00" E with an elevation of 85m above sea level.

To be able to get pristine data of surface water properties (30cm depth) all, in the field possible, measurements have been conducted. The maximum water depth, determined by a hand echolot, is about 7m, whereas the maximum water visibility, determined using a Secchi disc is 3.5m. Measurements with the WTW Multi 350i showed a redox potential [mV] of -20.1, a conductivity of 47 $\mu\text{S}/\text{cm}$ ($T_{\text{Ref}} 25^\circ\text{C}$), an acidity of 0.2 mmol/l and a pH-value of 7.18. The hydrochemical data surveyed by Moritz Kausche is displayed in Table 4. The ion balance resulted in a value of 11.2 mg/l.

Table 4: Hydrochemistry of sampled surface water, * marks concentration below the detection limit (data Moritz Kausche, 2008).

Al	Ba	Ca	Fe	K	Mg	Mn	Na	P
[mg/l]	[mg/l]	[mg/l]	[mg/l]	[mg/l]	[mg/l]	[mg/l]	[mg/l]	[mg/l]
200	< 20*	5.67	442	0.28	2.25	<20*	0.59	<0.1*

Si	Sr	F ⁻	Cl ⁻	SO ₄ ⁻	Br ⁻	NO ₃ ⁻	PO ₄ ⁻	HCO ₃ ³⁻
[mg/l]	[mg/l]	[mg/l]	[mg/l]	[mg/l]	[mg/l]	[mg/l]	[mg/l]	[mg/l]
0.18	<20*	<0.05*	0.57	0.26	<0.05*	<0.15*	0.24	19.1

The 33.0cm long short core, which was already sampled in the field, was obtained at a waterdepth of 4.8m. No cryoturbation typical structures were observed during the sampling of the core, which makes it most unlikely that the lake freezes completely during wintertime.

4.2 Results of pollen data and spectra composition

4.2.1 General characteristics of the pollen spectra

47 pollen samples were counted throughout the core. From sample 1 to 26 each sample was analysed, to get a resolution as high as possible. Starting from sample 26 to 58 at least every second sample has been counted.

40 different pollen species have been identified. *Potamogeton* has been excluded from further statistical analyses, as it represents an aquatic species and this study focuses on terrestrial taxa. Since a threshold of a minimum appearance in at least three samples accounting for at least 0.5% was set in this thesis to ensure a statistical relevance of the species, the following 17 taxa were excluded:

Caltha, Chenopodiaceae, c.f. Dipsacaceae, Fabaceae, c.f. Gentianaceae without porus, *Geum*-type, *Juniperus*, *Lysimachia vulgaris*-type, *Rumex acetosa*-type, Saxifragaceae, Scrophulariaceae, Solanaceae (Solanum), *Thalictrum*, *Triglochin*, *Trollius*, *Tsuga*, *Ulmus*.

The following results refer to the 22 species, which occurred on a regular basis throughout the short core and are displayed in Figure 15.

Pollen percentages of tree and shrub taxa are dominating the pollen assemblage and vary between 52.7% and 82.6%, averaging at 60.5% (n= 47). *Betula nana* -type is the most common and accounts for an all sample mean of 31.7% with a minimum at 20.8% and a maximum of 39%. *Alnus* has been found to have the second highest tree percentage with a minimum of 10.5% and a maximum of 29.3%, displaying the highest values in the upper three samples and showing an overall average of 15.9%. The highest values of *Larix* (median 8.2%) are present in the upper most samples as well, whereas pollen percentages throughout the core vary between 4.4% and 18%. Although Ericales show a relatively low mean of 2.3%, they show a high variability and account for at least 0.5% of the entire pollen assemblage, but reach up to 6.9% in the middle part of the short core.

Herb pollen vary throughout the core between 17.4% in the upper samples and 47.3% in the middle section (mean at 31%). Cyperaceae (mean of 20%) and Poaceae (mean of 8.4%) reach their lowest values in the first (Cyperaceae 9.6%) or second (Poaceae 5.1%) sample and display their maxima with a combined percentage of 44.7 in the middle core section, thereby dominating the pollen composition. Herb taxa, which are pollinated by insects display distinctly lower pollencounts, e.g. Ranunculaceae (0 - 1.2%, average of 0.4%) and Caryophyllaceae (0 - 1.3%, mean of 0.6%).

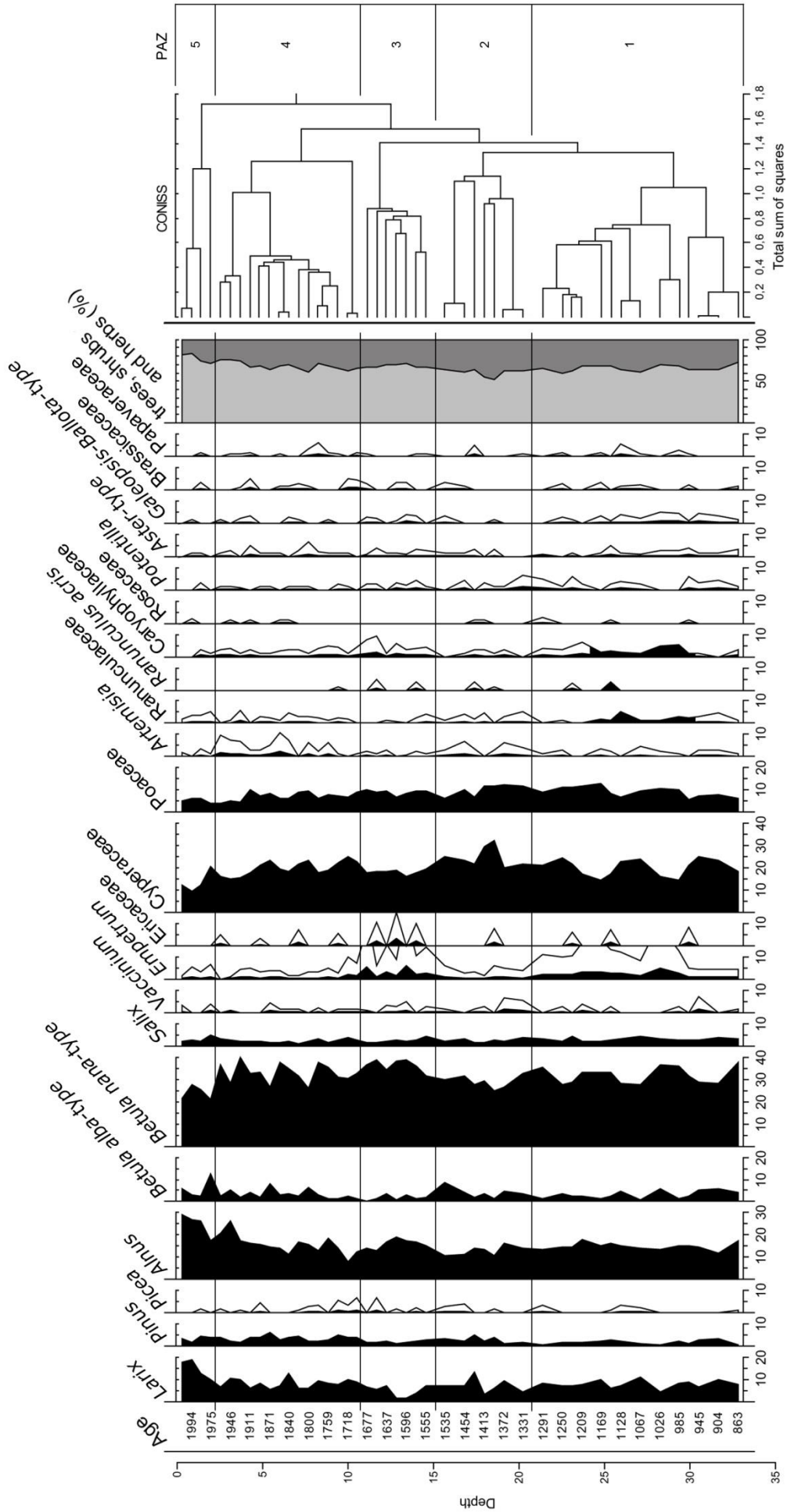


Figure 15: Pollen diagram of the 47 short core samples. Depth and age are (AD); all even ages shown due to legibility) shown on the left hand side. Taxa are given in percentages of all terrestrial pollen. Rare taxa (n=15) with an appearance of less than 0.5% in 3 out of 47 samples are excluded from this diagram. Results of the CONISS analysis are displayed on the right hand side.

4.2.2 Cluster analysis

All 22 taxa shown in Figure 15 are included in the cluster analysis progressed with CONISS. The obtained results are also shown in Figure 15.

CONISS revealed the following cluster and has led to a classification of five sections:

Pollen assemblage zone (PAZ) 1 includes the lower 13 samples (58-38) reaching from 33.0cm – 20.5cm of depth. This zone is characterized by rather high percentages of Cyperaceae and *Betula nana*-type pollen, as well as *Larix* pollen, but is not displaying any trend.

PAZ 2 spans the samples 36 to 28 at a depth of 20.5cm – 14.8cm. This zone shows a slight decrease of *Alnus* and *Betula nana*-type, still high Cyperaceae and Poaceae and relatively high *Artemisia* percentages.

PAZ 3, which reaches from 14.8cm to 10.8cm, grouping samples 26-20, is characterized by a precise decrease in *Larix* as well as *Betula alba*-type pollen and an increase of *Betula nana*-type and Ericales pollen.

PAZ 4 identifies the samples 19 to 5, at a depth of 10.8cm to 2.3cm, as statistically associated. The main characteristics of this PAZ are the pronounced increase of *Alnus* pollen as well as the decreasing Ericales pollen percentages and the slowly lowering Cyperaceae and Poaceae percentages.

PAZ 5 contains the four upmost samples and reaches down to a depth of 2.3cm. This zone displays a rapid increase of *Larix* and *Alnus* pollen and is furthermore characterized by low Cyperaceae and Poaceae percentages.

4.2.3 Ordination analysis

As the preliminary ascertained results for the DCA show a gradient length of 0.73 standard units, it is possible to choose a linear response model for the data set.

The first axis of the PCA illustrated 22.2% of the total variance of the data set. Combined with the second axis (13.9%) 36.1% of the variance are explained. Results of the species centred DCA and PCA are shown in Table 5 and Table 6.

Table 5: Results of the detrended correspondence analysis (DCA) performed on pollen data (n=47) from lake 07-SA-34.

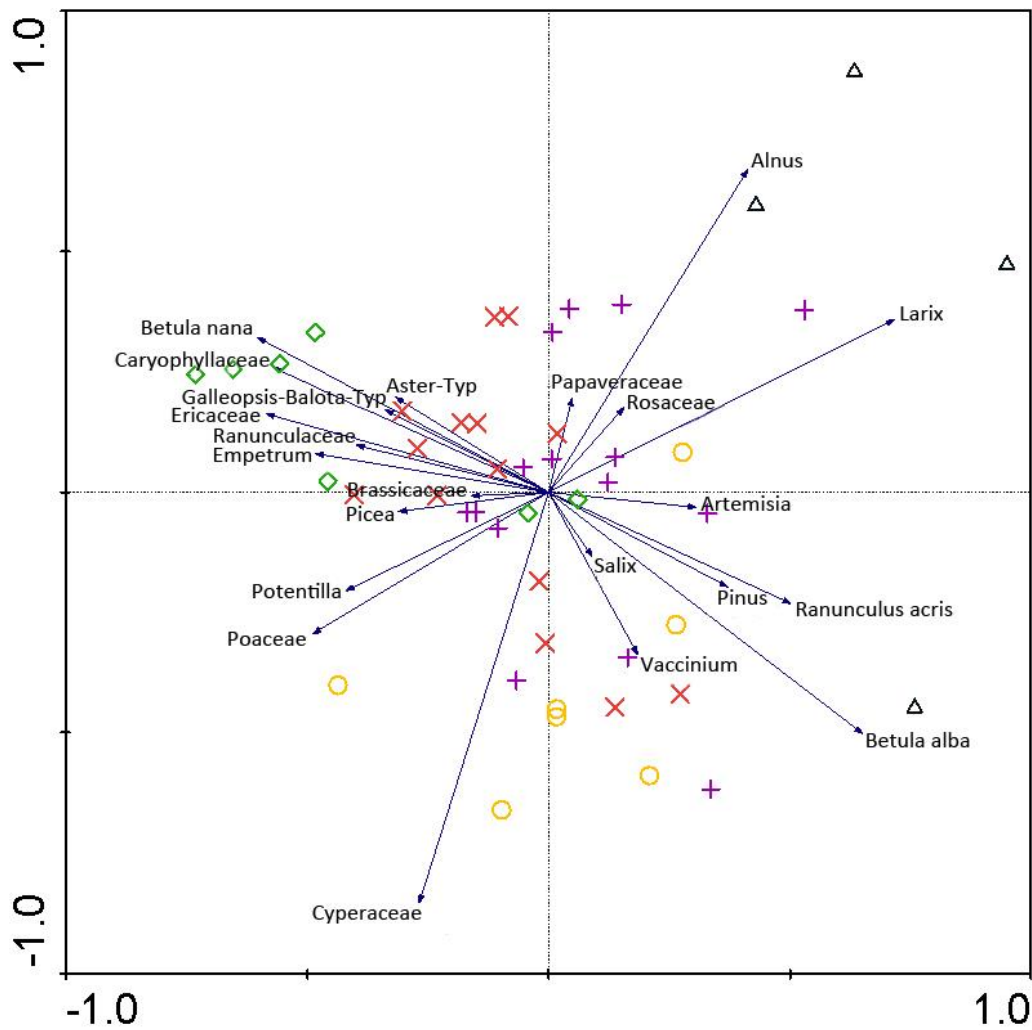
<i>Axis</i>	<i>Eigenvalue</i> λ	<i>Length of</i>	<i>Cumulative variance</i>
		<i>gradient</i> <i>sd</i>	<i>of species data</i> %
1	0.053	0.732	27,2
2	0.018	0.500	36.6
3	0.014	0.504	43.6
4	0.008	0.500	48.0

Table 6: Results of the principal component analysis (PCA).

<i>Axis</i>	<i>Eigenvalue</i> λ	<i>Cumulative variance</i>
		<i>of species data</i> %
1	0.222	27.2
2	0.139	36.1
3	0.120	48.1
4	0.088	56.9

The diplot shown in Figure 16 displays the results of the PCA. The five zones defined by the cluster analysis are reflected in the diagram. PAZ 3 and PAZ 5 plot clearly in relation to the first axis, whereas PAZ 1, 2 and 4 are more widely spread. In regard to the second axis PAZ 1 shows the clearest signal and is almost completely located in the negative quadrants.

Alnus and *Larix* are located in the positive quadrants of both axes and explain most samples of PAZ 5. In combination with *Betula alba*-type, which also plots positively on the first axis but negatively on the second axis, the dominating species of the samples of PAZ 5 are explained. Many herb and shrub taxa, which contribute in large parts to the PAZ 3, plot positively on the second axis, but negatively on the first axis, thereby displaying a contrast to PAZ 5. Grass and sedge protrude into the negative quadrant of both axis and seem to have an influence, together with *Vaccinium* on the plotting of the majority of samples of PAZ 1.



				
Zone 5	Zone 4	Zone 3	Zone 2	Zone 1

Figure 16: PCA, displaying the first two axes for the short core 07-SA-34.

4.2.4 Pollen concentration and influx

The mean pollen concentration resulted in about 35,000 grains per square centimetre, displaying a high of ~79,000 grains/cm² and a low of ~16,000 grains/cm². Pollen grain influx rates per year vary strongly with depth. There are three phases, where high influx rates occur. The first phase located at about 22-19cm depth, the second one at approx. 14-12cm of depth (maximum of ~1,900 grains/a) and the last one covering the upper three centimetres of the core. The most pronounced core section with relatively low influx rates reaches from 11 to 5cm of depth, showing a minimum value of ~540 grains/a at about 8cm.

Betula nana-type and *Alnus* influx rates show similar patterns, with varying values for *Betula nana*-type from 83 to 382 grains/a (averaging at 183 grains/a) and *Alnus* from 39 to 381 grains/a (median at 158 grains/a).

The influx rates of *Larix* (median at 77 grains/a) show on average slightly higher values in the lower part of the core, but decrease towards the upper part (minimum at 20 grains/a) and increase in the upper 5cm drastically (maximum at 262 grains/a).

Concentration values and influx rates of the pollen spectrum as well as influx rates of assorted species are displayed in Figure 17.

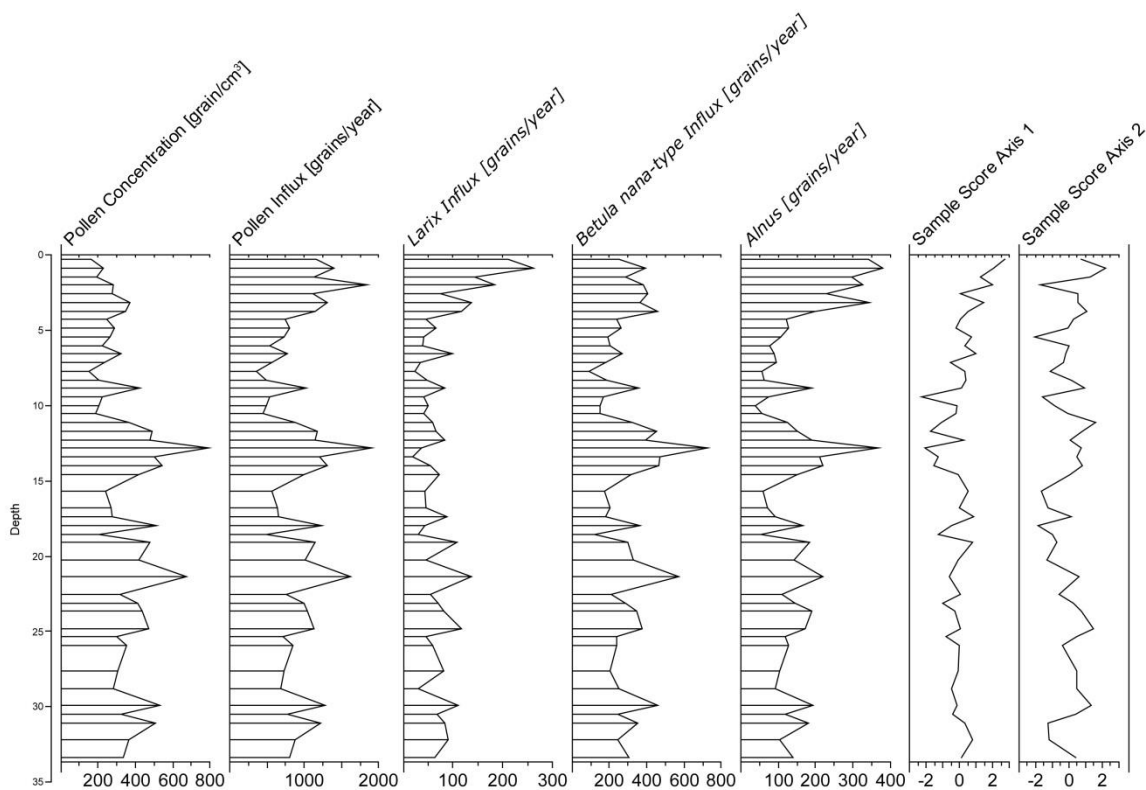


Figure 17: Pollen concentration and pollen influx diagram for the entire pollen composition, *Larix*, *Betula nana* and *Alnus* and sample Scores of Axis 1 and 2.

4.3 Results of grain size analyses

The grain size determination shows that the sediment within the short core 07-SA-34 is poorly sorted (Figure 18). As gravel and coarse sand are absent from the core, the grain size classes consist of clay, silt and sand. There are no severe changes of grain size distribution visible throughout the core. Clay ($< 2\mu\text{m}$) presents, with a mean of 14,7%, the smallest portion of the

sediment and ranges from 10.4% to 20.3%. Sand represents the second largest fraction and ranges from 4.6% to 30.6%, showing an average of 15% . Furthermore the distribution curves of sand and clay show a similar development. Silt ($> 2\mu\text{m}$ and $< 63\mu\text{m}$) clearly dominates the grain size distribution with a maximum of 78.6% (at 11.12cm depth) and a minimum of 61.3% (at 20.24cm depth). A mean of 70.3% of all the sediment is counted towards silt, as is visualised in the sediment triangle according to Shepard (Figure 19). The only occurring classes are sandy silt, clayey silt and silt, which are all characterised by a minimum appearance of 50% silt. The results are included in Figure 20. For an overview of the results of the grain size dermination please check the appendix Table A.1.

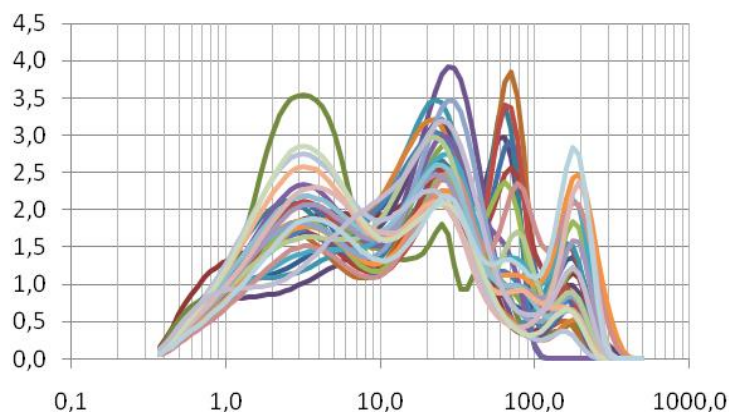


Figure 18: Grain size distribution of short core 07-SA-34, showing the poorly sorted character of the sediment throughout the core.

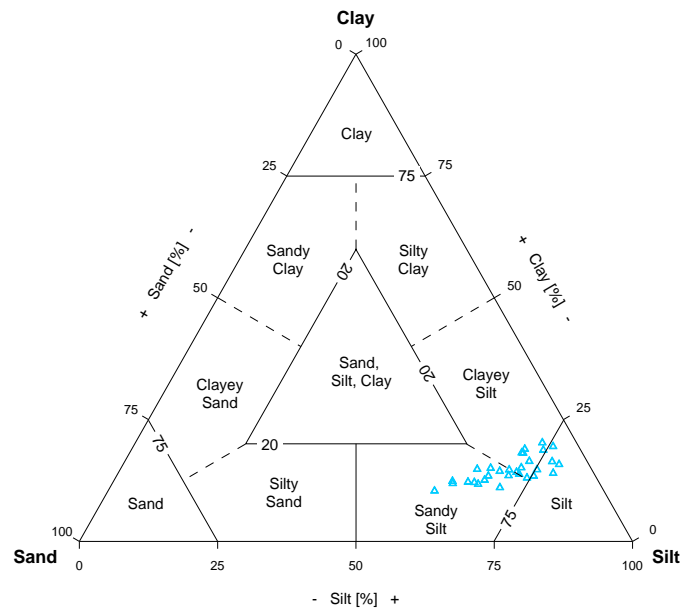


Figure 19: Sediment triangle after Shepard (1954) with grain size data of core 07-SA-34.

4.4 Results of biogeochemistry

Analyses of total nitrogen (TN), total carbon (TC) and total organic carbon (TOC) reveal a distinct variation throughout the core. The measured concentrations of TN, TC and TOC, as well as the calculated values of TIC and the TOC/TN ratio are displayed in Figure 20 and compiled values can be found in Table A.1 in the appendix.

TN values were determined between 0.17 to a maximum of 0.60% and an average of 0.34%. From about 870 to 1500 AD the measurements showed a negative trend, with a short rise in TN values around 1050 AD, ranging from 0.52 to 0.29%. The lowest values occur from approx. 1500 to 1700 AD, whereas the absolute minimum is reached at a depth of 11.12cm (1670 AD). After 1700 AD a strong increase in TN concentration is noticeable. This positive trend intensifies even more around the year 1911 AD (represented by a depth of 4.28cm) and still continues in 1994 AD (sample depth of 0.86cm), when the last measured sample was dated.

TC as well as TOC show very similar developments in their concentration values.

Concentrations of TC reach from 2.15 to 6.58%, with a mean of 3.85%. The minimum was once again determined around 1670 AD (sample depth 11.12cm) and was followed by a rapid increase in concentration throughout the rest of the core.

The distribution of TOC follows that of TC, presenting a minimum of 1.96% and a maximum of 5.54%. Calculated TIC values show percentages between 0.17 and 1.04 and are thus relatively low.

The ratio of TOC (%) to TN (%) averages at 10.2 and ranges from 8.03 to 12.93, showing only slight variations. In this study the lowest values are determined between the years ~1400 to 1550 AD and once more lowering from ~1700 to 1994 AD, the latest contained data.

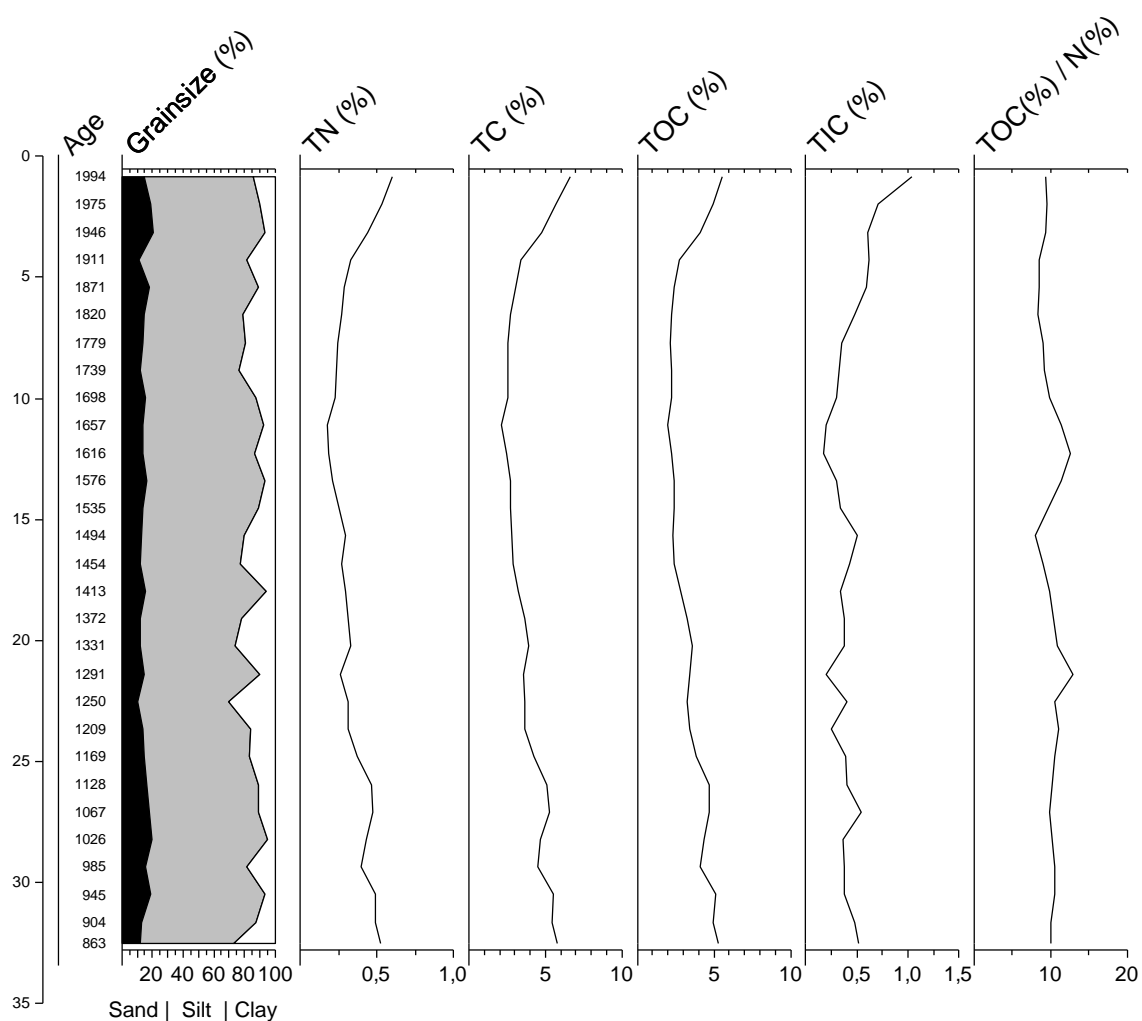


Figure 20: Results of grain-size distribution, total nitrogen (TN), total carbon (TC), total organic carbon (TOC), total inorganic carbon (TIC), all in % as well as the TOC and TN ratio.

4.5 Results of stable isotope geochemistry ($\delta^{13}\text{C}_{\text{org}}$, $\delta^{15}\text{N}_{\text{Total}}$)

The $\delta^{13}\text{C}$ isotope ratios of organic carbon range from -32 to -28‰. The lowest rates are found in the lower part (~900 to 1150 AD) and in the upper part (~1900 to 1994 AD) of the short core. After a rapid increase, starting at about 1460 AD, the maximum value is reached around 1620 AD and the $\delta^{13}\text{C}$ value starts to decrease strongly afterwards. The $\delta^{13}\text{C}$ isotopic ratio averages -30.1‰ consistently through the core.

The $\delta^{15}\text{N}$ isotope ratios display values from 2.6‰ to 3.7‰ showing a clear positive trend, whereas the lowest ratios are located in the bottom samples (~860 AD) and the highest are at

about 1870 AD. The median lies at 3.2 ‰ for all samples. Figure 21 visualises $\delta^{13}\text{C}$ and $\delta^{15}\text{N}$ isotope ratios. Results can be inspected in Table A.2 in the appendix.

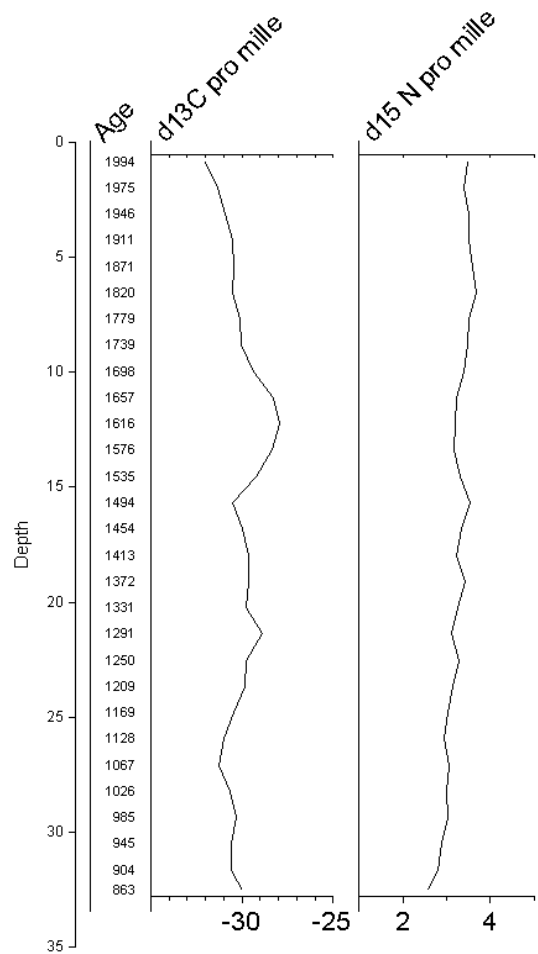


Figure 21: Isotopic ratios of $\delta^{13}\text{C}$ and $\delta^{15}\text{N}$.

4.6 Age-depth-model

The age-depth-model is based on Pb/Cs measurements as reported by Appleby and Piliposyan (2010) and Drevens (2011). The age-depth-model for the upper 10 samples is displayed in Figure 22.

As it can be expected from the exponential nature of a sediment core, the ^{210}Pb dates were quite distinctive. A constant sedimentation, at least lasting since the beginning of the 20th century was identified by the generated dating models (Appleby and Piliposyan, 2010). The indicated mean sedimentation rate during this period lay at $0.011 \pm 0.001 \text{ g/cm}^2 \cdot \text{a}$, which equals a mean of 0.045 cm/a. The error lays at $\pm 7.1\%$.

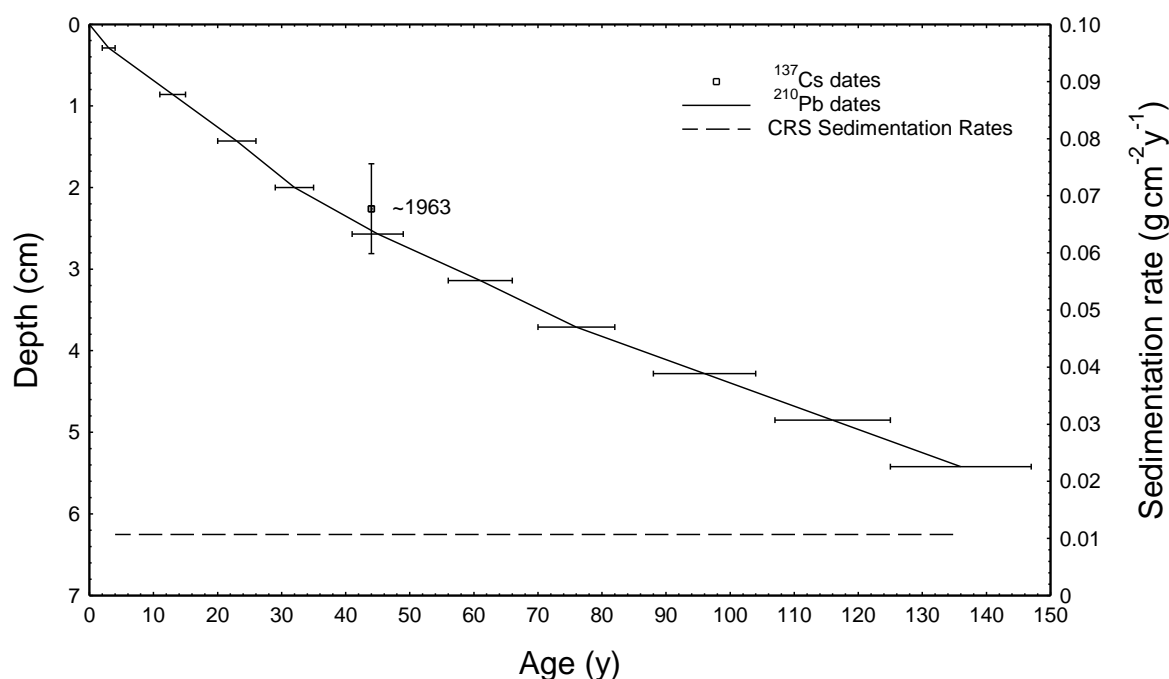


Figure 22: Age-depth-model of the upper centimeters, Radiometric chronology of the sediment core 07-SA-34 showing the ^{210}Pb dates and sedimentation rates as well as the approx. 1963 depth suggested by the ^{137}Cs record (report by Appleby and Piliposyan, 2010).

To verify that the sedimentation progressed at a constant level, three ^{14}C measurements were commissioned by the Leibniz Laboratory for Age Determination and Isotope Research at the Christian-Albrechts-University in Kiel. Sample 05, 37 and 56 of the 07-SA-34 core were determined. The leaching residue and the humid acid fraction were ascertained, showing older data for the leaching residue as for the humid acid fraction. Since leaching residue is less sensitive towards relocated carbon, their data was used to compile the age-depth-model (Dreves, 2011). The dating of sample 07-SA-34 05 was used to calculate the reservoir effect of the ^{14}C measured samples in comparison to the Pb/Cs dating. The reservoir effect in the short core 07-SA-34 amounts to 2108 years and was subtracted from the leaching residue values. Sample 07-SA-34 37 fits well into the age-depth reconstruction displayed in Figure 23. Unfortunately sample 07-SA-34 56 indicates a much too young age. This can occur, when younger material is transported into the sample or if the reservoir effect varies strongly in different depths. The ^{14}C age determination results are shown in the age-depth model, but are considered less reliable and were therefore not used to construct the age-model of the lower part of the core.

As a constant sedimentation throughout the upper samples of the core suggests a sedimentation rate, that levels out at approx. 0.028 cm/a, this rate was assumed to be valid for

the entire core. The merged figure of the Pb/Cs dating, as well as the assumed sedimentation rate and the ^{14}C dating is shown in Figure 23.

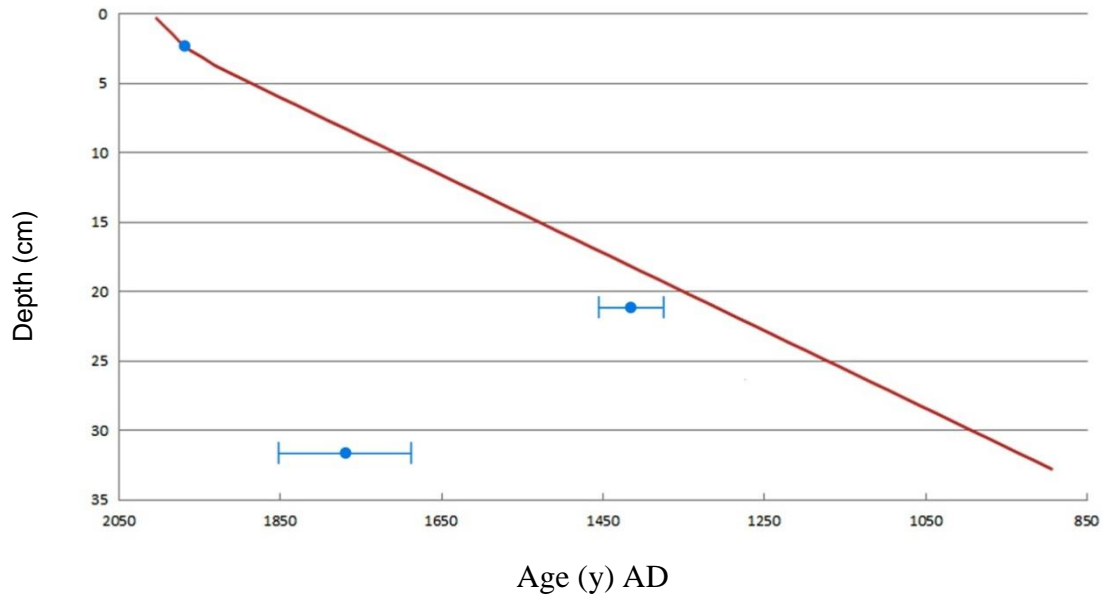


Figure 23: Age-depth-model; the Pb/Cs dating results as well as the assumed sedimentation rates are shown in red. The ^{14}C dating results with the range of error (1σ range) are shown in blue.

5 Discussion

5.1 Vegetation change during the last 1100 years (From Yakutia to the entire Arctic)

5.1.1 Pollen source area and productivity reconstruction

To be able to make predictions about future vegetation developments in climate change sensitive zones, it is necessary to understand the vegetation changes of the past.

Fossil pollen assemblages are well suited as a primary source of information for past vegetation compositions and changes from decadal to millennial timescales (Jackson and Lyford, 1999). In 1963, Davis already stated that “the theoretical relationship between vegetation percentage and the percentage of pollen in the sediment makes it obvious that where species differ in the amounts of pollen they contribute to sediments”, it is necessary to consider this while interpreting pollen assemblages.

It has been well known, that the signal displayed in the pollen composition depends on the size of the lake itself (Sugita, 1993). Small lakes are known to be dominated by local vegetation pollen, whereas pollen assemblages from larger lakes are more influenced by regional spectrum vegetation. Depending on the lakes size, the ratio between local and regional pollen in the sediment and therefore the source area can differ strongly (Davis, 2000). Many studies undertaken in Northern Siberia are based on pollen records retrieved from small thermokarst ponds or polygon mires, which reflect mainly the local vegetation or on the other hand are based on records from very large lakes like the Labaz lake (470 km²) (Andreev et al., 2001) or the Lama lake (466 km²) (Hahne and Melles, 1997), which are displaying a mainly regional vegetation signal and far more long-distance transported pollen than small lakes. The investigated lake 07-SA-34 covers an approx. area of 600 m times 300 m, and is therefore expected to reflect a more regional pollen signal.

Furthermore, it has to be mentioned, that pollen grains from different species found in the lake sediment have different sized source areas, due to variations in their morphology (Sugita, 1993). Some species, like *Larix*, produce rather large and heavy pollen grains and it can therefore be assumed that the source area is located close to the deposition area. Sugita (1993) e.g. showed that about 50% of the *Larix* pollen found in a lake with a diameter of 250 m originate from a

1,000 m radius around the lake center. Other pollen grains, which are considerably lighter, e.g. *Alnus* or *Salix*, would, under the same conditions, represent a source area of an approx. 10,000 m radius (50%) around the lake (Sugita, 1993). Again other species, which are well known as long-distance components are *Pinus* or *Picea*, which possess air sacs to support their weight. These specific characteristics enable the pollen grains to overcome large distances and settle far away from their original distribution area (Birks and Birks, 1980). It is most likely that the *Pinus* and *Picea* grains displayed in the pollen spectra of lake 07-SA-34, reached their final deposit area by long-distant transport, as their range of distribution in Central Siberia does not reach up this far north. These pollen grains are so called overrepresented. Whether the dispersion is regional or local is depending on factors like a) turbulence of the atmosphere, b) wind speed and direction, c) terminal falling velocity (depending on shape and size of the pollen grain) and d) height and strength of the pollen source (Birks and Birks, 1980). It is generally accepted that pollen record from lakes in the high latitudes are often more influenced by long-distance transported pollen due to a limited pollen production of the local vegetation in response to cold climate and the harsh living conditions. Furthermore, it has to be taken into account, that a certain amount of species found in the study region are insect-pollinated species. These produce a far lower amount of pollen than wind-pollinated species (e.g. Birks and Birks, 1980) and it is therefore hard to detect a pronounced signal of these species in the pollen record. Wind-pollinated taxa, like Cyperaceae and Poaceae, which are the dominating species in the pollen diagram of this study, produce a large amount of pollen.

5.1.2 Vegetation change inferred from pollen data

The short core pollen spectrum from the investigated lake, shown in Figure 15 was previously (see chapter 4.2.2) subdivided into five pollen assemblage zones (see chapter 4.2.2), which will be discussed in this chapter.

In the lower part of the core, pollen assemblage zone (PAZ) one, which lasts until the end of the 13th century is rather homogenous with small variations in the main taxa *Betula nana*-type and *Alnus*. Cyperaceae and Poaceae, the two dominating herb taxa throughout the core, contribute a large part to the PAZ 1. Despite the variations in the percentages of *Larix* and *Betula alba*-type pollen grains, both occur in considerable numbers, indicating the Medieval Warm Period. This

warmer period was also found in pollen records e.g. by Andreev and Klimanov (2000) in Northern Siberia.

The here generated pollen diagram shows little variations between the pollen assemblage zones one and two (spanning a time from the beginning of the 14th to the middle of the 16th century), which leads to the assumption that zone two also shows the Medieval Warm period but starts to reflect slightly decreasing temperatures towards the end of this warmer period.

It becomes apparent that the *Larix* pollen percentage, which represents the dominating tree taxa, reaches its minimum within the short core in the pollen assemblage zone three, which lasts from the middle of the 16th century until the middle of the 18th century. During the same time a distinct rise of Ericales pollen grains as well as an increase of herb pollen such as Caryophyllaceae occurs, leading to the assumption that the treeline retreated during this time, since the mentioned shrubs and herbs prefer open habitats. Subally and Quézel (2002) are deriving from modern *Artemisia* ecology and habitat investigations that no generalized habitat preferences towards warmer or cooler, or wetter or drier conditions can be postulated for *Artemisia*. Regardless these doubts, *Artemisia* is yet obviously displaying a lower appearance in the PAZ 3 than in the adjacent PAZ 2 and 4, indicating changes in the climatic conditions during that time. All together the pollen composition leads to the assumption, that PAZ 3 reflects the so called 'Little Ice Age' (LIA), which was mentioned in other pollen studies as well, e.g. Andreev et al. (2002), and Bradley and Jones (1993), who reconstructed the LIA from pollen records in the northern central USA. Several studies (e.g. Grace et al.2002, MacDonald et al.1993; MacDonald and Case, 1998; MacDonald et al.2007) postulate a coherence between treeline changes and climate. MacDonald et al. (2007) argue that the limits of the treeline in the northern Arctic are defined by the short and cool growing season in the high latitudes and even though the growing season would permit some taxa to survive, the winter temperatures play an important role as well, as some species are prone to bud and needle damage by harsh weather conditions, such as blowing snow and ice (MacDonald et al.2007). Larch, a deciduous Pinaceae, for example defines the treeline in northern Central Siberia, where mean January temperatures reach up to below -30 degrees. The treeline in Fennoscandia, on the other hand, a region where winter temperatures range around -10 to -15 degrees, is mainly composed of pine and birch (MacDonald et al. 2007).

In between the rather variable PAZ 3 and PAZ 5, another more nonspecific pollen composition, PAZ 4 with a higher percentage of tree pollen, as well as an increase in e.g. Ranunculaceae and *Aster-typ* pollen percentages indicates a slight rise of temperature.

The upper and therefore most recent samples, displayed in PAZ 5, provide the clearest and most distinct signal throughout the short core. Starting around 1970 a distinct increase in *Larix* pollen both in percentages and in deposition rate, as well as a rather higher percentage of tree birch and elder, coinciding with a decreasing number of herb pollen and the knowledge of the modern day vegetation suggests the presumption that the treeline moved back northwards, and that the tree density and height in the lakes vicinity increased. *Larix* pollen percentages up to 18.9% are quite remarkable, as *Larix* pollen are usually not as well represented in pollen records. Clayden et al. (1996) for example presented a study in which larch pollen only represented 8% of the pollen spectra composition, although the surveyed sediment was retrieved from a lake located within a larch forested catchment. Clayden et al. (1996) state, that *Larix* is strongly underrepresented.

The diplot visualizing the PCA (Figure 16) may show similar findings. It can be suggested, that the 1st axis is reflecting the development of the vegetation from southern tundra to forest-tundra and northern taiga. This assumption is based on the distribution of the taxa in the PCA, since the open-habitat preferring species plot with negative values in comparison to treelike species, which plot positive values on the 1st axis. It can furthermore be concluded, that the 1st axis is displaying changes in the treeline and therefore reflects a temperature signal.

The 2nd axis does not show an equally pronounced signal, but it might be indicating differences concerning the local soil moisture. It is not likely that a regional signal is indicated. Cyperaceae, which dominate the signal on the 2nd axis, probably reflect changes in the lakes vicinity, which are not climatically induced. A higher water level or waterlogging in the lakes shore areas, due to changes in the morphology because of thermokarst developments or a rising permafrost table, which would prohibit the drainage of the area, could infer possible explanations.

5.1.3 Vegetation response to climate signals and feedbacks

Pollen spectra based findings of this thesis match reconstructions of vegetation and climate within the last millennia in the Arctic regions. The Medieval Warm Period as well as the Little Ice

Age integrate into the general Holocene cooling trend in the Northern Hemisphere, e.g. shown for Scandinavia by Karlén and Kuylenstierna (1996) or North East European Russia by Salonen et al. (2011). The general cooling trend itself is not reflected in the short core sediment, due to its limited length and reach back in time.

Dahl-Jensen et al. (1989) are showing distinct temperature developments during the MWP and the LIA by means of the GRIP Ice core and the Dye 3 for the Greenland region. It can be assumed however that the reconstructed climate events occurred, in different peculiarities, in most regions in the high-latitudes, respectively. Similar reconstructions were published by Opel (2009) using stable water isotopes from the Akademii Nauk ice cape (Severnaya Zemlya, Russia). This study illustrates low $\delta^{18}\text{O}$ values, indicating cooler conditions, around 1500 AD as well as around 1780 AD. The values are rising strongly at the end of the 19th century and although dropping slightly after approx. 1970 AD a noticeable trend is displayed towards Global Warming.

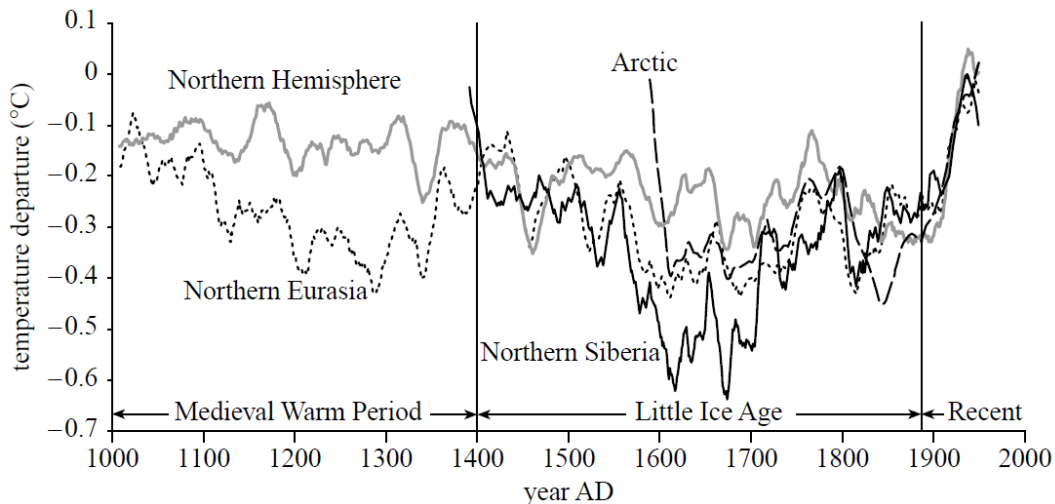


Figure 24: Northern Hemisphere, Arctic, Northern Eurasian and Northern Siberian summer surface-temperature trend over the past 1000 years (MacDonald et al.2008).

Dendrochronological analyses, published and combined by MacDonald et al. (2000; 2008) among others, are suggesting that the MWP and LIA were distinct in all of the Northern Hemisphere as well as Northern Siberia (Figure 24).

As modern day climate change progresses, it is most likely, that also the treeline in the northern hemisphere will move northwards. In the past, e.g. during the Holocene Climate Optimum in the Boreal (starting around 9200 B.P.), the treeline stretched supposedly to the current coast of the Arctic ocean, as many, mainly dendrochronological and pollen based studies are showing (Figure 25) (e.g. Andreev and Klimanov, 2000; Hahne and Melles, 1997; MacDonald et al.2000).

These studies are also coinciding in the reconstruction of the treeline retreat between 3000 to 4000 years BP, presumably mainly due to of declining of summer insolation and cooling arctic waters (MacDonald et al.). Up to now, the former limits of the treeline have not been reached (Figure 25) but if global warming continues at its current pace, it is most likely to do so in the near future.

However, it appears that the vegetation in northern Central Siberia is out of equilibrium in regard to the recorded temperature rises in the last century. It can be assumed that the main reasons are the low production of fertile grains, due to harsh climate conditions and also the low possibility to fall onto a well suited ground and germinate. This presents, especially in the southern tundra, where a thick groundcover of mosses and lichen can impede a successful germination, an obstruction (Walter, 1990). Esper and Schweingruber (2004) state, that the local tree recruitment is not only related to temperature variations, but also dependent on micro-site conditions, insect outbreaks, wintertime snow and wind conditions and grazing pressure. This also might explain the visible time-lag in the distribution of e.g. *Larix*, in the here presented pollen record. At some locations in the Northern Hemisphere Subarctic no treeline movement occurred in the last century, although higher temperatures were measured. This, however, is not the norm, as treeline advances and structural changes in the vegetation cover are recorded e.g. in Scandinavia, Quebec and the Canadian Rocky Mountains (Fritz and Schweingruber, 2004).

A further northward moving treeline could have a positive feedback on global warming as well. Especially in the north Siberian regions, albedo is high during most of the year due to snow cover and the generally higher radiation of tundra compared to the forest-tundra. If evergreen tree species such as pine and spruce are expanding on the expense of the deciduous larch, albedo values would decrease and could enhance global warming further (MacDonald 2007).

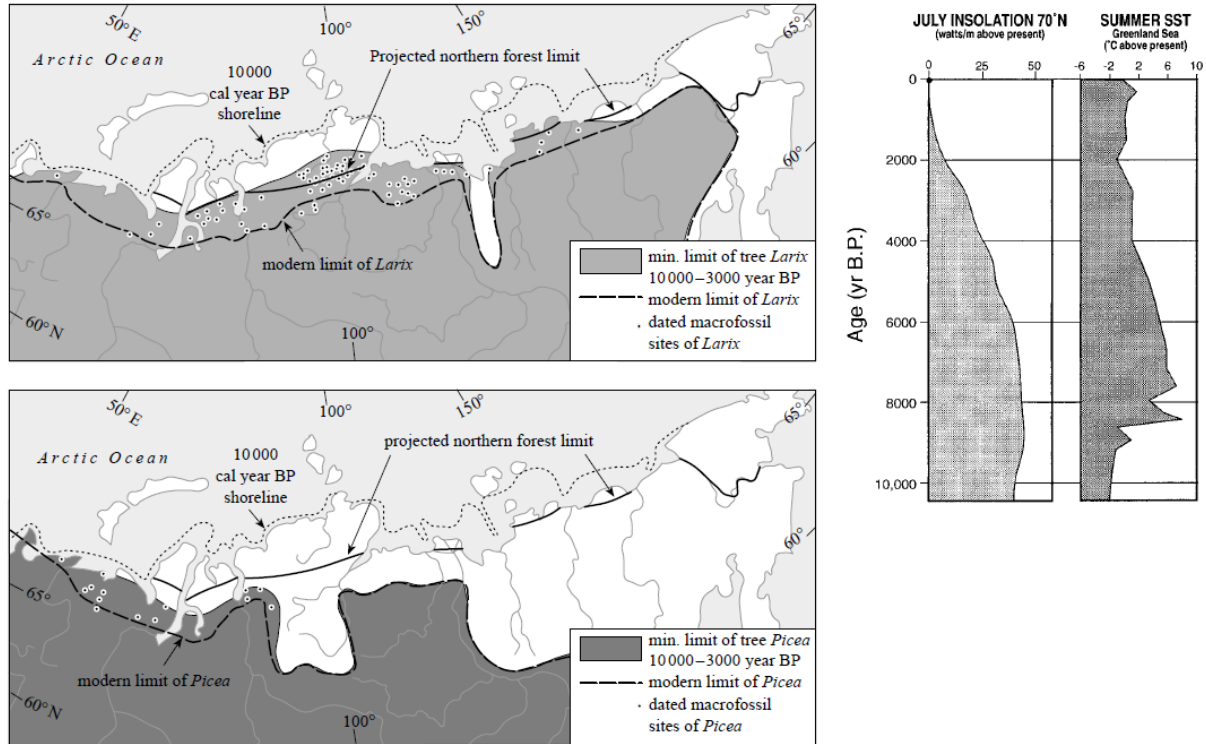


Figure 25: a) Projected position of the treeline in late twenty-first century (according to ACIA 2004), current northern limits of trees (top-*Larix*; bottom-*Picea*), Holocene Thermal Maximum northern treeline limits based upon the distribution of radiocarbon dated wood and b) July insolation at 70° and summer sea surface temperatures in the Greenland Sea reconstructed on the base of diatoms (extracts from MacDonald et al.2000 and MacDonald et al.2008).

5.2 Changes in the environmental setting of the north Siberian lake 07-SA-34

In Northern Eurasia there are almost three million lakes to be found, the majority of which, 98% in particular, are less than 1km² in size (Koronkevich, 2002). In the northern European territory, the Western and northern Central Siberia are, according to Koronkevich (2002), the moisture supply as well as the widespread topographic depressions, which are both associated with periglacial landforms, the main reasons for the formation of lakes. Lake 07-SA-34 is, as are the most lakes in the area of Northern Siberia (Koronkevich, 2002), a pronounced thermokarst lake and water availability and topography are the two main factors that control the lake regime.

Signals from pollen spectra appear often smoothed and reflect the environment on a more regional scale and do not necessarily coincide with signals shown by in-lake investigations (Wischnewski et al. 2011, Dalton et al. 2005). Hence, the following part will concentrate on the within lake development in order to gain a comprehensive picture of environmental evolution during the last millennium.

In order to be able to make assumptions about former environment settings and compositions of lake systems a multi-proxy approach is often used, as the influential factors are usually not only reflected in one sedimentological parameter (Wischneswkie et al. 2011, Xu et al. 2006). This thesis was therefore compiled as a multi-proxy study, including grain size distributions, biogeochemical and stable isotope measurements and supplementary water analyses results (by Kausche 2008).

Grain size distribution is recognized as an often used tool to reconstruct the predominating energy regimes in lake systems (Last, 2001). It also enables us to gain information about the sedimentary input at the time of deposition. As thermokarst lakes in northern Central Siberia are developing under specific conditions, such as a high volume of ground-ice, widespread river terraces with fine-grained alluvial material etc. and since the area remained ice-free throughout the Quaternary and acted as sediment trap, large amounts of alluvial sediments accumulated in the region in the past (French, 2007). High temperature differences in the area are assisting the formation of thermokarst lakes, since warm summer temperatures can reflect in a deep reaching active layer (French, 2007). In the Arctic, most of the biological and physical processes are taking place in the active layer (Hinzmann et al. 1991; Kane et al. 1991). Therefore, the development of thermokarst lakes, the resulting talik as well as the geomorphic changes are affecting the surrounding environment. Because of the close relationship and interaction of the thermal and hydrological regime it is predictable that changes in one parameter will result in changes of the entire system (Hinzmann et al. 1991).

As already mentioned in chapter 4.3 cluster the grain size measurements in the area of sandy to clayey silt (silt >50%) and pure silt (silt >75%). Most of them are containing more than 70% silt and show little variation through the core. This indicates that the sedimentary environment in the lake was rather stable (Cohen, 2003) and the pollen signals were not disturbed by changes in the lake morphology or fluvial input. Furthermore, this supports the assumption that the

sedimentation rate did not strongly change throughout the core, which indicates the reliability of the proposed age-depth-model.

The grain size signal displayed in the core may reflect on the one hand the sediment composition of the area in general, but on the other hand may describe the sediment distribution at one point within the lake only, and may therefore be considered biased, as the grain size distribution on the lake shore is likely to show a different spectra (Birks and Birks, 1980; Füchtbauer, 1974). For palaeolimnological studies it is common practice to sample lakes in the deepest or otherwise the central part of the lake, in order to gain an as undisturbed signal as possible (Birks and Birks, 1980). Here, in turn, the smallest grain size is expected, as the energetic regime is lowest in this part of the lake, which allows smaller particles to settle and deposit (Birks and Birks, 1980). The total organic carbon (TOC) given in dry weight % is, to a certain degree, depending on the composition of the sediment. A higher amount of clastic material, generally found in close proximity to the lake shore, can dilute the TOC, just as a decrease of lateral sediment supply can lead to an increase on TOC values (Meyers and Teranes, 2001). Thompson and Eglinton (1978) are showing that, as the grain size decreases, the TOC concentration increases. This leads to the assumption that the investigated material from the center part of the lake 07-SA-34 most probably also contains an elevated TOC concentration.

In this study TOC was determined as bulk values and therefore represents the amount of organic matter that reached the sediment surface after its transportation through the water column where it was potentially altered or partly remineralized (Meyers, 2003). Organic matter can either originate from the remains of phyto- and zooplankton, algae, bacteria and aquatic higher plants (Meyers and Teranes, 2001) or it can enter the lake via the run-off or fluvial input from the surrounding areas. The signal reflected in the sediment core can therefore be autochthonous or allochthonous dominated, but due to low precipitation rates as well as the thick absorptive vegetation layer (see chapter 2.5 and 2.6) it is most likely that a mainly autochthonous signal is displayed in this study. It may therefore be assumed that the presented TOC and TN values reflect the productivity of the lake, as the TOC/TN ratio is considered a well suited proxy for the origin of organic matter in lake sediments (e.g. Meyers, 1994; Meyers and Teranes, 2001). Hereby it is of great use that the TOC/TN ratio of nonvascular plants, e.g. phytoplankton, differs strongly from the TOC/TN ratio of vascular plants such as grass, shrub and trees. Vascular, or other terrestrial plants display a ratio of about 20 or larger, phytoplankton on the other hand

generally reveals ratios between 4 and 10 (Meyers and Ishiwatari, 1993). All TOC/TN ratios in this study indicate towards a phytoplankton dominated signal in the sediment with some organic matter originating from terrestrial C₃ plants, visualized in Figure 26.

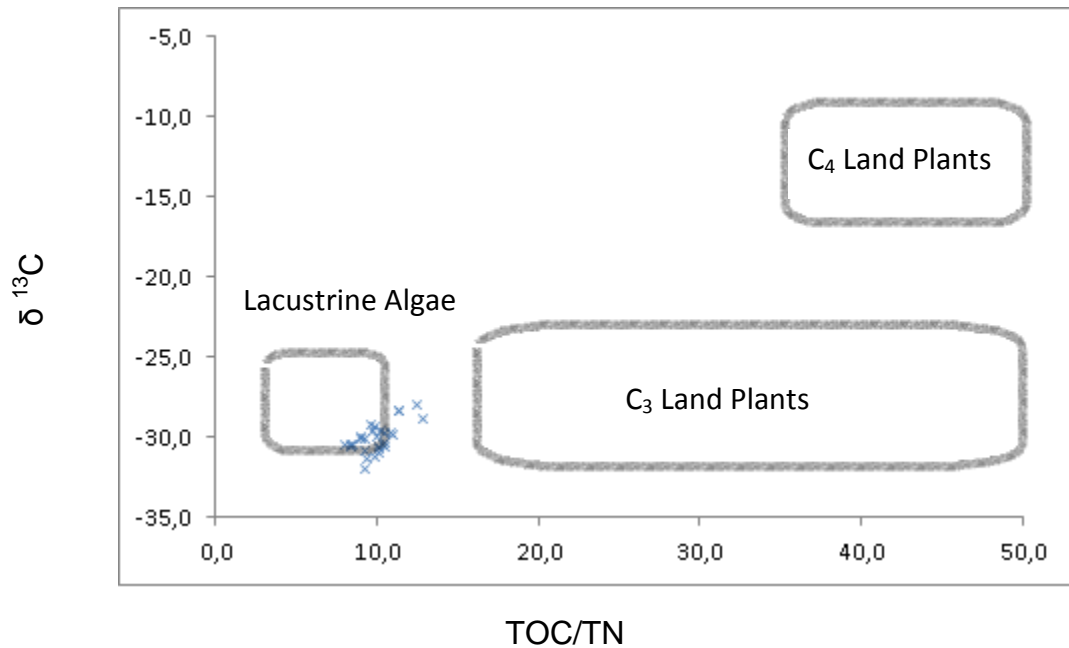


Figure 26: Elemental and carbon isotopic composition of lake samples. Scheme after Meyers (1994).

Meyers and Teranes (2001) are pointing out, that the two main influencing factors of the TOC concentration in the sediment are the initial production of biomass as well as the subsequent degree of degradation, thereby storing multiple information, such as the origin of the organic matter, depositional processes and the amount of preservation.

The results of this study are showing higher values during the, from the pollen spectra composition derived, warmer periods (MWP and the 20th century) and a decrease of the TOC concentration during the colder phase (LIA). It can be assumed that the TOC, combined with the total nitrogen, fluctuates with the bioproductivity of the lake system. Hereby cause warmer temperatures an increase of bioproductivity and colder temperatures a decrease. During the colder phase, the ice cover on the lake would thicken and a prolonged ice-coverage would result in a shortening of the productivity period for in situ living plants, algae and phytoplankton, which are the primary source of organic matter. Animal remains contribute only a few percent to the

organic matter according to Meyers and Lallier-Vergès (1999). During the beginning of the 20th century a distinct increase in TOC as well as TN is shown in the measured data, indicating a still rising bioproductivity, which can be assumed to reflect the modern date climate change.

Another often used proxy for reconstructing productivity rates as well as the availability of nutrients in lakes, are stable isotopes (Meyers and Teranes, 2001). In this study $\delta^{13}\text{C}$ and $\delta^{15}\text{N}$ values were determined as bulk values of the organic matter.

The $\delta^{13}\text{C}$ results show significant trends within the core, see Figure 21. If applicable, a differentiation of C₃ to C₄ plants can be made based on $\delta^{13}\text{C}$ values, as plants use different pathways to incorporate carbon into their organic matter. However it is not likely that the $\delta^{13}\text{C}$ values are affected by C₄ plants, as there are almost no C₄ plants to be found in the study area, but taxa with these metabolism concentrate in warm-arid areas as the C₄ metabolism is an adaptation to water limitation (Fischer and Turner, 1978).

Due to fraction, C₃ plants reflect a relatively low $\delta^{13}\text{C}$ ratio with an average of about -27‰ (e.g. Meyers, 1994; Smith and Epstein, 1971). These values are nevertheless not fixed, particularly not for aquatic plants such as submerged vascular plants or algae, as they can assimilate hydrogen carbonate in addition to dissolved carbon dioxide. Water organisms would, under normal circumstances, prefer the incorporation assimilation of dissolved CO₂ (Bade et al. 2006) which, due to effective fractionation results in light isotope values. However, during phases of CO₂ limitation, e.g. during phases of high bioproductivity or phases of increased pH-levels, HCO₃⁻ becomes an important carbon source, which results in heavier $\delta^{13}\text{C}$ values (Meyers and Teranes, 2001). Using diatom analyses, Laing et al. (1999) found that pH values are relatively high in tundra areas due to poor soil development in combination with high soil weathering rates, which result in an increased input of minerals as source of base cations. In forested areas the pH values are generally lower, because of changes in the organic acid influx, which results in a changing acid and base cation ratio in the lake system. A high input of leaf-litter, especially composed of *Larix*, a deciduous conifer species and the dominating tree in Northern Siberia, would provide an important source of humic acids for the lake system (Laing et al. 1999). Modern limnological investigations in the Lena River area showed, that changes in alkalinity can be interpreted as an indicator for a retrieving treeline in the study area (Duff et al. 1999). Hence, it can be expected that the pH-level would decrease, if the vegetation around the lake changes from tundra to forest-

tundra and relatively more CO₂ in comparison to HCO₃⁻ would be dissolved in the lake water and be available to water-living organisms, which is recordable in lower δ¹³C values.

Consistently with this conceptual model, the highest pH-values can be reconstructed around the 16th to 17th century, where the pollen-based vegetation reconstruction indicates a treeline retreat probably caused by the LIA temperature minimum. During the MWP and the present Global Warming relatively low pH-values could be reconstructed for the determined δ¹³C values.

In addition to the relationship described above, a prolonged ice coverage in the wintertime during the LIA might even have enhanced the limitation of dissolved CO₂, forcing water-living organisms to use the remaining heavier δ¹³C.

This assumption is furthermore supported by the results reflected in the δ¹⁵N measurements. Although not standardized in paleolimnological studies, δ¹⁵N compositions are a useful proxy for identifying the origin of organic matter in sediment and reconstructing bioproductivity rates, just as δ¹³C (correlation shown in Figure 27) (Meyers, 2003). It is yet difficult to distinguish the different signals that compose the δ¹⁵N values, as they are dependent on many factors. In general, plankton is showing heavier δ¹⁵N values (about 8‰), using the most common dissolved nitrogen, NO₃⁻, in the lake water. Land plants on the other hand mainly use atmospheric N₂, which exhibits a δ¹⁵N value of 0‰ (Meyers and Teranes, 2001). The measured results of the examined lake show a mixed signal, if, as is suggested, the δ¹⁵N values estimate the origin of the organic matter. It seems only natural that some remains of C₃ land plants are compound into the sediment. This is also reflected in the slightly higher TOC/TN values than common for a pure lacustrine algae signal. A minor positive trend is recognizable in the δ¹⁵N curve, with a slight dissent during the Little Ice Age. This again could be induced by several factors. Meyers (1994) states that a higher abundance of nitrogen fixing cyanobacteria can decrease the δ¹⁵N in the sediment, which was probably induced by less mixing as a result of a prolonged ice-coverage. Since the changes in δ¹⁵N are not very large, it is also probable that they are caused by a change in phytoplankton species composition or an increase of heterotrophs, as the δ¹⁵N is increase with each trophic transfer (Meyers and Teranes, 2001).

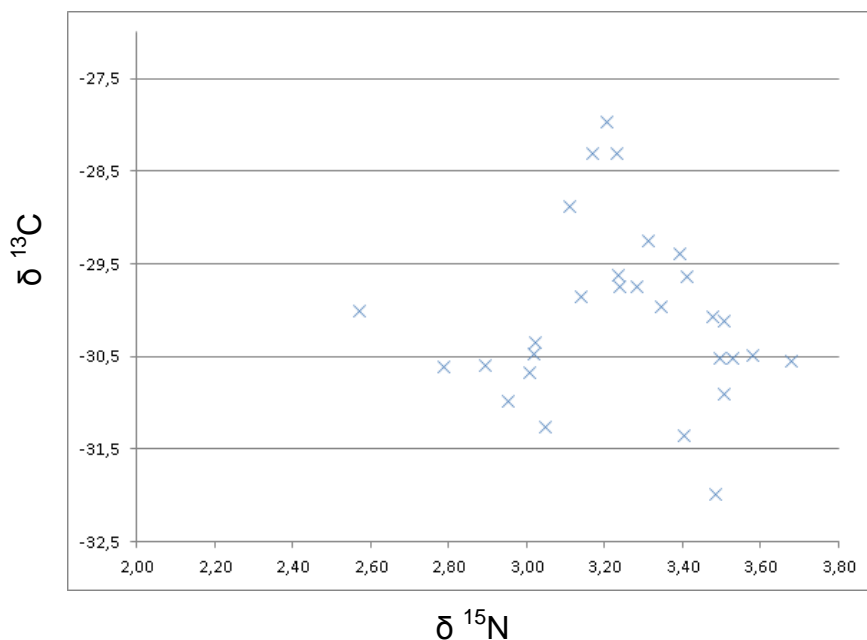


Figure 27: Nitrogen and carbon isotopic composition of lake samples.

Taking the pollen spectra composition during the Little Ice Age into account, it is also likely that the decrease in the $\delta^{15}\text{N}$ originated from a higher input of land plants with lower $\delta^{15}\text{N}$ values, as different tundra plants show different $\delta^{15}\text{N}$ values. Nadelhoffer et al. (1996) postulate that Ericales and *Betula nana*, which are both more common during the LIA, e.g. show a smaller $\delta^{15}\text{N}$ ratio than willow and sedge, which decrease during colder phases. It is furthermore possible that changes towards colder conditions have a general effect on the $\delta^{15}\text{N}$ composition as shown by Hodell and Schelske (1998), who are postulating a 6‰ $\delta^{15}\text{N}$ difference that occurs between summer and wintertime in the sediment of Lake Ontario, Canada, due to different sedimentation rates that can occur during periods of mixing or stratification of the watercolumn and the increased production of organic matter during blooms.

A generalized explanation for fluctuations in $\delta^{15}\text{N}$ values is hard to find, as the nitrogen cycle is very complex and influenced by many factors. However, it is possible to interpret the positive trend in the $\delta^{15}\text{N}$ curve as an overall increase in productivity in lake 07-SA-34, which is likely to increase further if vegetation periods stretch, due to climate change and rising temperatures in the Arctic.

Considering the holistic approach, it can be assumed that lake 07-SA-34 underwent the typical development of a thermokarst lake in the high Arctic. According to the sequences of development of alas thermokarst relief, after French (2007), pictured in Figure 07, it can be assumed that the lake is currently residing in stage 3b to 3c. During these stages of thermokarst development, a larger depression has already formed and a rather flat bottom with a thermokarst lake has developed, as unfrozen sediment breaks of the sides of the alas and accumulates. It is most likely that the lake has reached its maximum dimension and will start to shrink, due to aggradation or a development of drainage systems (French, 2007). Nevertheless, the results presented here indicate that external climate signals are well preserved in the investigated lake, though overprinted by the long-term internal development.

5.3 Limitation of data set and possible enhancements

Pollen and geochemical proxies and their modern analogues are widely used to reconstruct past climates and environmental changes (e.g. Birks and Birks, 1980; Meyers and Lallier-Vergès, 1999). However, it is necessary to be aware of the limitation and qualification of the surveyed data. Pollen grains for example are produced in unequal quantities by different taxa and vary in their distribution areas, e.g. due to pollination-type, pollen grain production, climate variability, pollen grain morphology etc. Another limitation is given in the constraint, that pollen are mainly determined on a family level and rarely on a species level, which may lead to false interpretations as single species may have different habitat requirements. It is also difficult to distinguish between the pollen grain input of the local vegetation and regional or even supraregional vegetation, and difficulties concerning the precise determination of the source area still exist.

In this study a successive counting of all remaining pollen samples would complete the short core record and might underline the thus far discovered result. Additionally stomata counts could help to increase the knowledge about the proportion of pollen grains in comparison to the occurrence of the taxa in the area. Furthermore, a detailed analysis of non pollen polynomorphs would be desirable in order to support ones findings concerning the local environment as well as the lake itself.

Moreover, it has to be taken into account, that only one short core was investigated in this study. In order to gain more precise results and to rule out interpretations of punctual displayed signals, further short cores from lake 07-SA-34 could be determined. If the research goal was to extend or intensify the research of vegetation changes (treeline movement) in regard to Global Warming, further investigations of different lakes in the region would be needed. It would be useful if the studied lakes would be selected along a transect across the treeline, to be able to determine the recent movement of the treeline and to compare the data with records of previous climate changes.

These further investigations should also include the determination of geochemical proxies, as they can also be useful to determine changes in the environmental parameters in the lakes vicinity. As shown, it is more likely that the geochemical analyses conducted in this study indicate mainly lacustrine signals, rather than local or regional changes in the lakes environment. However it becomes clear that a multi-proxy approach is very valuable if one aims at understanding the entire system 'lake' and its determining parameters.

6 Conclusion

A multi-proxy approach was applied in order to reconstruct the development and impacts of changes in the environmental setting of the lake in northern Central Siberia, as well as changes in the vegetation cover in the surrounding area. The aim of this study was to identify these changes and draw conclusions regarding the climatic changes in the area as the high latitudes are exceptionally sensitive to temperature changes.

A total of five pollen assemblage zones were identified within the short core, each distinguished by a different pollen species composition. However, the most pronounced and therefore significant PAZ were one, three and five. Hereby

- the oldest part of the core, PAZ 5, is representing the Medieval Warm Period, ending around 1320 AD,
- PAZ 3, is reflecting the Little Ice Age, lasting from 1550 to 1670 AD and
- the four upmost samples are showing the contemporary effects of Global Warming.

Since no clear signals could be identified, PAZ 2 and 4 were classified as transition zones.

Some distinct changes within the sedimentary results could be detected and were used to reconstruct former environmental parameters. Especially the biogeochemical analyses are showing higher values in the lower part of the core, which gradually decrease until the end of the LIA and start increasing again around 1650 AD to reach their maximum levels in the surface sample. This is most likely reflecting a lower bioproductivity during the sedimentation of the middle part of the core and as higher bioproductivity rates in the lower and the upper part, thereby showing a warmer phase in the oldest and in the youngest parts and a colder phase in the middle section.

The combination of biogeochemical (TOC) and stable isotope ratio ($\delta^{13}\text{C}$) analyses enables us to draw the conclusion, that the signals preserved in the organic matter of the sediment are mainly lacustrine signals and do not reflect changes in the lake's terrestrial vicinity.

The reconstructed and in this study discussed results of the pollen record as well as the measured sedimentary results are displaying similar climatic signals, proving the multi-proxy approach to be useful, as many proxies can be inferring different interpretations.

The following conclusions can be drawn:

- 1) Warmer conditions shaped the vegetation and in-lake developments from about 900 to 1550 AD.
- 2) The often postulated LIA is recorded in the sediment of the lake and clearly found in pollen assemblage, reaching its climax approx. at the turn of the 16th century.
- 3) Increasing treepollen percentages and a pronounced trend in sedimental signals coincide with the modern day climate change and the accompanying rapid rise of temperatures.

It must be expected that, if the modern day climate change progresses at its current rate, the treeline in the circum-arctic regions will move further northwards, thereby decreasing the albedo and increasing the solar heating of land. This is most likely to promote a positive feedback, which will result in even higher temperatures and considerable changes in the environment of the high latitudes.

Taking predicted temperature rises, treeline movement and the general lake development into account, certain changes in the vegetation, including aquatic and terrestrial taxa, are to be expected, not only changing the composition of the lake system itself, but also the environmental parameters in the lakes vicinity.

7 References

- ACIA (2004). Impacts of a warming Arctic: Arctic Climate Impact Assessment. Cambridge University Press. Cambridge.
- Andreev, A.A. and Klimanov, V.A. (2000). Quantitative Holocene climatic reconstruction from the Arctic Russia. *Journal of Palaeolimnology* 24, pp.81-91.
- Andreev, A.A., Siegert, C., Klimanov, V.A., Derevyagin, A.Y. and Shilova, G.N. (2002). Late pleistocene and Holocene Vegetation and Climate on the Taymyr Lowland, Northern Siberia, *Quaternary Research* 57, pp. 138-150.
- Appleby, P.G., Nolan, P.J., Gifford, D.W., Godfrey, M.J., Oldfield, F., Anderson, N.J. and Battarbee, R.W. (1986). ^{210}Pb dating by low background gamma counting. *Hydrobiologia* 141, pp. 21-27.
- Appleby, P.G. and Piliposyan, G.T. (2010). Report on the radiometric dating of the lake sediment core 07-SA-34 from the Yakutia region of Siberia.
- Bade, D.L., Pace, M.L. Cole, J.J. and Carpenter, S.R. (2006). Can Algal photosynthetic inorganic carbon isotope fractionation be predicted in lakes using existing models? *Aquatic Science* 68, pp.142-153.
- Beug, H.J. (2004). Leitfaden der Pollenbestimmung für Mitteleuropa und angrenzende Gebiete. Verlag Dr. Friedrich Pfeil, München, p. 542 ff.
- Birks, H.J.B. and Birks, H.H. (1980). Organic sediments in palaeoecology. In: *Quaternary Palaeoecology*. London, Edward Arnold (Publishers) Limited. pp.46.ff.
- Birks, H.J.B. and Birks, H.H. (1980). Principles and methods of pollen analysis. In: *Quaternary Palaeoecology*. London, Edward Arnold (Publishers) Limited. pp.156.ff.
- Blackmore, S., J.A.J. Steinmann, P.P. Hoen & W. Punt (2003). Betulaceae and Corylaceae. Review of Paleobotany and Palynology 123, pp. 71-98.

- Bonan, G.B. (2008). Forests and Climate Change: Forcing, Feedbacks, and the Climate Benefits of Forests. *Science* 320, pp. 1444-1449.
- Bottomley, R., Grieve, R., York, D. and Masaitis, V. (1997). The age of the Popigai impact event and its relation to events at the Eocene/Oligocene boundary. *Nature* 388, pp. 365-368.
- Bradley, R.S. and Jones, P.D. (1993). 'Little Ice Age' summer temperature variations: their nature and relevance to recent global warming trends. *The Holocene* 3, pp. 367-376.
- Chernov, Y.I. and Matveyeva, N.V. (1997). Arctic ecosystems in Russia. In: Wielgolaski, F.E. (Ed.), *Ecosystems of the World 3: Polar and Alpine Tundra*. Elsevier, Amsterdam, pp.361-507.
- Chester, P.I. and Ian, R.J. (2001). Pollen and spore keys for Quaternary deposits in the northern Pindos Mountains, Greece. *Grana* 40, pp. 299-387.
- Clayden, S.L., Cwynar, L.C. and MacDonald, G.M. (1996). Stomate and pollen content of lake surface sediment from across the tree line on the Taimyr Peninsula, Siberia. *Canadian Journal of Botany* 74, pp.1009-1015.
- Cohen, A.S. (2003). *Paleolimnology - the History and Evolution of Lake Systems*. Oxford University Press, Oxford, p.162 ff.
- Craig, H. (1953). The geochemistry of the stable carbon isotopes. *Geochimica et Cosmochimica Acta* 3, pp. 53-92.
- Dahl-Jensen, D., Mosegaard, K., Gundestrup, N., Clow, G.D., Johnson, S.J., Hansen, A.W. and Balling, N. (1998). Past Temperatures Directly from the Greenland Ice Sheet. *Science* 282, pp.268-271.
- Dalton, C., Birks, H.J.B., Brooks, S.J., Cameron, N.G., Evershed, R.P., Peglar S.M., Scott, J.A. and Thompsen, R. (2005). A multi-proxy study of lake-development in response to catchment changes during the Holocen at lochnagar, north-east Scotland. *Palaeogeography, Palaeoclimatology, Palaeoecology* 221, pp.175-201.
- Davis, M.B. (1963). On the Theory of Pollen Analysis. *American Journal of Science* 261, pp.897-912.

- Davis, M.B. (2000). Palynology after Y2K – understanding the source area of pollen in sediments. *Annual Reviews of Earth and Planetary Science* 28, pp. 1-18.
- Degens, E.T. (1969). Biogeochemistry of Stable Carbon Isotopes. In: Eflinton, G., Murphy, M.T.J. (Eds.), *Organic Geochemistry: Methods and Results*. Springer, Berlin.
- de Klerk, P., Donner, N., Joosten, H., Karpov, N.S., Minke, M., Seifert, N. and Theuerkauf, M. (2008). Vegetation patterns, recent pollen deposition and distribution of non-pollen palynomorphs in a polygon mire near Chokurdakh (NE Yakutia, NE Siberia). *Boreas* 38, 1.
- Drevers, A. (2011). Datierungsergebnisse der Schnellproben KIA 4472-44744, 44746-44748, 44751.
- Duff, K.E., Laing, T.E., Smol, J.P. and Lean, D.R.S. (1999). Limnological characteristics of lakes located across arctic treeline in northern Russia. *Hydrobiologia* 391, pp.205-222.
- Esper, J. and Schweingruber, F.H. (2004). Large-scale treeline changes recorded in Siberia, *Geophysical Research Letters* 31, L06202.
- Fægri, I. and Iversen, J. (1989). *Textbook of Pollen Analyses*. 4th Addition, John Wiley and Sons, Chichester, p.328 ff.
- Fischer, R.A. and Turner N.C. (1978). Plant Productivity in the Arid and Semiarid Zones. *Annual Reviews Plant Physiology* 29, pp.277-317.
- French, H.M. (2007). *The periglacial environment*. 3rd Addition, John Wiley and Sons, Chichester.
- Füchsbauer, H. (1974). *Sediments and Sedimentary Rocks 1*. E.Schweizerbart'sche Verlagsbuchhandlung (Nägele und Obermiller), Stuttgart, p.51 ff.
- Grace, J., Berninger, F., Nagy, L. (2002) Impacts of Climate Change on the Tree Line. *Annals of Botany* 90, pp.537-544.

- Grimm, E.C. (1987). CONISS: a FORTAN 77 programm for statistically constrained cluster analysis by the method of incremental sum of squares. *Computer & Geoscience* 13, pp. 13-35.
- Hahne, J. and Melles, M. (1997). Late- and post-glacial vegetation and climate history of the southwestern Taymyr Peninsula, central Siberia, as revealed by pollen analysis of a core from Lake Lama. *Vegetation History and Archaeobotany* 6, pp.1-8.
- Håkanson, L. and Jansson, M. (2002). *Principles of lake sedimentology*. Blackburn Press, Caldwell, New Jersey.
- Handbook Elementar Vario EL III (2001). Elementar Analysensysteme GmbH. Hanau.
- Handbook Coulter LS Series Teil III (1993). Coulter Electronics GmbH. Krefeld.
- Hicks, S. and Hyvarinen, H. (1999). Pollen influx values measured in different sedimentary environments and their palaeoecological implications. *Grana* 38, pp. 228-242.
- Hinzmann, L.D., Kane D.L., Gieck, R.E. and Everett, K.R. (1991). Hydrologic and thermal properties of the active layer in the Alaskan Arctic. *Cold Regions Science and Technology* 19, pp.95-110.
- Hodell, D.A. and Schelske, C.L. (1998). Production, sedimentation, and isotopic composition of organic matter in Lake Ontario. *Limnology and Oceanography* 43, pp. 200-214.
- International Arctic Science Committee (Lead Author); Peter Saundry (Topic Editor) "Arctic Climate Impact Assessment (full report)". In: *Encyclopedia of Earth*. Eds. Cutler J. Cleveland (Washington, D.C.: Environmental Information Coalition, National Council for Science and the Environment). [First published in the *Encyclopedia of Earth* February 5, 2010; Last revised Date December 20, 2010; Retrieved July 27, 2011 <[http://www.eoearth.org/article/Arctic_Climate_Impact_Assessment_\(full_report\)>](http://www.eoearth.org/article/Arctic_Climate_Impact_Assessment_(full_report)>)
- IPCC (2007). *Climate Change 2007: The Physical Science Basis*. Contribution of Working Group I to the Fourth Assessment Report of the Intergovernmental Panel on Climate Change. Cambridge University Press. Cambridge.

- Jackson, S.T. and Lyford, M.E. (1999). Pollen Dispersal Models in Quaternary Plant Ecology: Assumptions, Parameters, and Prescriptions. *The Botanical Review* 65, pp.40-72.
- Jackson, D.A., and Somers, K.M. (1991). Putting things in order: the ups and downs of detrended correspondence analysis. *American Naturalist* 137, pp. 704-712.
- Jones, A., Stolbovay, V., Tarnocai, C., Broll, G., Spaargaren, O., Montanarella, L., JRC - European Commission (2010). *Soil Atlas of the Northern Circumpolar Region*.
- Kane, D.L., Hinzmann, L.D., Zarling, J.P. (1991). Thermal response of the active layer to climatic warming in a permafrost environment. *Cold Regions Science and Technology* 19, pp.111-122.
- Karlén, W. and Kuylentierna, J. (1996). On solar forcing of the Holocene climate: evidence from Scandinavia. *The Holocene* 6, pp.359-365.
- Kausche, M. (2008). Limnological characteristics of Northern and Central Yakutian lakes (Siberia) – Physical and chemical properties of surface sediments and water samples, Diploma Thesis, Humboldt-University Berlin.
- Koronkevich, N. (2002). Rivers, Lakes, Inland Seas and Wetlands. In: Shagedanova, M. (Ed.), *The physical geography of northern Eurasia*. Oxford, Oxford University Press, pp.135-136.
- Koronovsky, N. (2002). Tectonics and geology. In: Shagedanova, M. (Ed.), *The physical geography of northern Eurasia*. Oxford University Press, Oxford, pp. 1–35.
- Laing, T.E., Rühland, K.M., Smol, J. P. (1999): Past environmental and climatic changes related to tree-line shifts inferred from fossil diatoms from a lake near the Lena River Delta, Siberia. *The Holocene*, pp. 547- 557.
- Lancer (2008). http://www.google.de/imgres?imgurl=http://upload.wikimedia.org/wikipedia/commons/3/36/Russland_Relief.png&imgrefurl=http://commons.wikimedia.org/wiki/File:Russland_Relief.png%3Fuselang%3Dde&usg=__KqW9nYlm1DBCuqZro2L9pWdma10=&h=1346&w=2100&sz=4015&hl=de&start=54&zoom=1&tbnid=RmacLC49_IEJ9M:&tbnh=126&tbnw=196&ei=dJQuTp6iIYz6sgayqJHxDw&prev=/search%3Fq%3Drussland%26hl%3Dde%26client%3Dfirefox-a%26hs%3D

3Dq0K%26sa%3DX%26rls%3Dorg.mozilla:de:official%26biw%3D1280%26bih%3D917%26tbn%26sch&itbs=1&iact=rc&dur=356&page=3&ndsp=26&ved=1t:429,r:11,s:54&tx=99&ty=81

- Langer, M. and Venzke, Jörg-Friedhelm (2006). Zur Entwicklung der Vegetationsperiode in Nordostsibirien in der zweiten Hälfte des 20. Jahrhunderts. *Polarforschung* 75, pp.91-100.
- Last, W.M., (2001). Texture Analysis of Lake Sediments. In: Last, W.M. and Smol, J.P. (Eds.). *Tracking Environmental Change Using lake Sediments. Volume 2: Physical and Geochemical Methods.* Kluwer Academic Publishers, Dordrecht, The Netherlands. p.41 ff.
- Lydolph, P.E. (1977). *Climates of the Soviet Union, World Survey of Climatology Volume 7.* Elsevier Scientific Publishing Company, pp. 71-115.
- MacDonald, G.M., Edwards T.W.D., Moser, K.A., Pienitz, R. and Smol, J.P. (1993). Rapid response of treeline vegetation and lakes to past climate warming. *Nature* 36, pp.243-246.
- MacDonald, G.M. and Case, R.A. (1998). A 538-Year Record of Climate and Treeline Dynamics from the Lower Lena River Region of Northern Siberia, Russia. *Arctic and Alpine Research* 30, pp.334-339.
- MacDonald, G.M., Kremenetski, K.V. and Beilmann, D.W. (2008). Climate change and the northern Russian treeline zone. *Philosophical Transactions of the Royal Society B: Biological Sciences* 363, pp.2285-2299.
- Masaitis, V.L. (2002). Popigai Crater: General Geology. In: *Impacts in Precambrian Shields (2002).* Heidelberg, Berlin, Springer, p.81 ff.
- Matveyeva, N.V. (1994). Floristic classification and ecology of tundra vegetation of the Taymyr peninsula, northern Siberia. *Journal of Vegetation Science* 5, pp.813-828.
- Meyers, P.A. (1994). Preservation of elemental and isotopic source identification of sedimentary organic matter. *Chemical Geology* 114, pp. 289-302.
- Meyers, P.A. (1997). Organic geochemical proxies of paleoceanographic, paleolimnologic, and paleoclimatic processes. *Organic Geochemistry* 27, pp. 213-250.

- Meyers, P.A. (2003). Applications of organic geochemistry to paleolimnological reconstructions: a summary of examples from the Laurentian Great Lakes. *Organic Geochemistry* 34, pp. 261-289.
- Meyers, P. A. and Ishiwatari, R. (1993). Lacustrine organic geochemistry – An overview of indicators of organic matter sources and diagenesis in lake sediments, *Organic Geochemistry* 20, pp. 867–900.
- Meyers, P. A. and Lallier-Verges, E. (1999). Lacustrine sedimentary organic matter records of late quaternary paleoclimates. *Journal of Paleolimnology* 21, pp. 345–372.
- Meyers, P. A. and Teranes, J. L. (2001). Sediment organic matter. In: W. M. Last and J. P. Smol (Eds). *Tracking Environmental Change Using Lake Sediments, Vol. 2: Physical and Geochemical Methods*, Boston, Kluwer Academic Publishers, pp. 239–269.
- Mitrofanov, G. L. and Taskin, A. P. (1994). Structural relations of the Siberian platform with its folded frame. *Geotectonics* 28, pp. 1–12.
- Moore, P.D., Webb, J.A. and Collinson, M.E. (1991). *Pollen analysis*. 2nd edition Blackwell Press, Oxford, p.216 ff.
- Nadelhoffer, K., Shaver, G., Fry, B., Giblin, A., Johnson, L. and McKane, R. (1996). ^{15}N natural abundances and N use by tundra plants. *Oecologia* 1007, pp. 386-394.
- Opel, T., Fritzsche, D., Meyer, H., Schütt, R. Ruth, U. and Fischer, H. (2009). Late Holocene climate change in the Central Russian Arctic – evidence from Akademii Nauk ice cape (Severnaya Zemlya). In: *Glacier and ground ice as archives of Late Holocene climate and environmental change in the Russian Arctic*, Thomas Opel 2009, Dissertation, Humboldt-University, Berlin.
- Pilkington, M., Pesonen, L.J., Grieve, R.A.F. and Masaitis, V.L. (2002). Geophysics and Petrophysics of the Popigai Impact Structure, Siberia. In: Plado, J. and Pesonen, L.J. (Eds.). *Impacts in Precambrian shields*, Springer, pp. 87-107.
- Przybylak, R. (2003). *The Climate of the Arctic*; Atmospheric and Oceanographic Sciences Library, Volum 26. Dordrecht, Netherlands, Kluwer Academic Publishers, p.152-153.

- Resources and Environment World Atlas II (1998). Russian Academy of Science, Institute of Geography, Ed.Hölzel, Vienna and IG RAS, Moscow.
- Rozen, O. M. (1995). Metamorphic effects of tectonic movements at the lower crust level: Proterozoic collision zones and terranes of the Anabar shield. *Geotectonics* 29, pp. 91–101.
- Saarnisto, M. (2001). Climate variability during the last interglacial-glacial cycle in NW Eurasia. Abstracts of PAGES – PEPIII: Past Climate Variability Through Europe and Africa, 2001
- Salonen, J.S., Seppä, H., Väiliranta, M., Jones, V.J., Self, A., Heillilä, M., Kultti, S., Yang, H. (2011). The Holocene thermal maximum and late-Holocene cooling in the tundra of NE European Russia. *Quaternary Research* 75, pp.501-511.
- Scheffer, F. and Schachtschabel, P. (2002). *Lehrbuch der Bodenkunde*. Heidelberg, Berlin, Spektrum.
- Serreze, M.C. and Barry, R.G. (2005). *The Arctic Climate System*; Cambridge Atmospheric and Space Science Series, Dressler, A.J., Houghton, J.T., Rycroft M.J., Cambridge University Press.
- Shagedanova, M. (2002). The climate at present and in the historical past, In: *The physical geography of northern Eurasia*, Shagedanova, M. (Ed.) , Oxford, Oxford University Press, pp. 70–102.
- Smith, B. N. and Epstein, S. (1971). Two categories of $^{13}\text{C}/^{12}\text{C}$ ratios of higher plants, *Plant Physiology* 47, pp.380–384.
- Soloviev, P.A. (1973). Thermokarst phenomena and landforms due to frost heaving in Central Yakutia, *Biuletyn Peryglacjalny* 23, pp. 135-155.
- Stockmarr, J. (1971). Tablets with spores used in absolute pollen analysis, *Pollen et Spores* 13, pp. 614-621.
- Stuiver, M. and Polach, H. (1977). Reporting of ^{14}C data. *Radiocarbon* 19 (3), pp. 355-363.

- Subally, D., Quénzel, P. (2002). Glacial or interglacial: *Artemisia*, a plant indicator with dual responses. *Review of Palaeobotany and Palynology* 120, pp. 123-130.
- Svendsen, J. I., Alexanderson, H., Astakhov, V. I., Demidov, I., Dowdeswell, J. A., Funder, S., Gataullin, V., Henriksen, M., Hjort, C., Houmark-Nielsen, M., Hubberten, H.-W., Ingólfsson, Jakobsson, M., Kjær, K. H., Larsen, E., Lokrantz, H., Lunkka, J. P., Lyså, A., Mangerund, J., Matiouchkov, A., Murray, A., Möller, P., Niessen, F., Nikolskaya, O., Polyak, L., Saarnisto, M., Siegert, C., Siegert, M. J., Spielhagen, R. F. and Stein, R.: 2004, Late Quaternary ice sheet history of northern Eurasia, *Quaternary Science Reviews* 23, pp. 1229–1271.
- ter Braak C.J.F. and Šmilauer, P. (2002). *CANOCO reference Manual and CanoDraw for Windows User's Guide, Software for Canonical Community Ordination (version 4.5)*. Mircocomputer Power, Ithaca, New York, USA.
- Tishkov, A. (2002). Boreal Forests, In: Shagedanova, M.(Ed.) *The physical geography of northern Eurasia*, Oxford, Oxford University Press, pp.216-233.
- Thompson, S. and Eglinton, G. (1978). The fractionation of a recent sediment for organic geochemical analysis. *Geochimica et Cosmochimica Acta* 42, pp. 199–207.
- Vishnevsky, S. and Montanari, A. (1999). Popigai impact structure (Arctic Siberia, Russia): Geology, petrology, geochemistry, and geochronology of glass-bearing impactites. *Geological Society of America, Special Papers* 339, pp.19-59.
- Voigt, I. (2009). *Spätquartäre Bodenwasserdynamik im Antarktischen Ozean südöstlich des Kerguelen-Plateaus*. Diploma thesis, University of Potsdam.
- Walter, Heinrich (1990). *Vegetation und Klimazonen*. Ulmer, Stuttgart, 6. Auflage, p.331 ff.
- Washburn, A.L. (1979). *Geocryology: a survey of periglacial processes and environments*. London, Edward Arnold.
- Washburn, A.L. (1980). Permafrost Features as Evidence of Climatic Change. *Earth-Science Reviews* 15, pp. 327-402.

Wischniewski, J., Mischke, S., Wang, Y. and Herzschuh, U. (2011). Reconstructing climate variability on the northeastern Tibetan Plateau since the last Lateglacial – a multi-proxy, dual-site approach comparing terrestrial and aquatic signals. *Quaternary Science Reviews* 30, pp.82-97.

Xu, H., Ai, L., Lai, L. and An, Z. (2006). Stable isotopes in bulk carbonates and organic matter in recent sediments of Lake Qinghai and their climatic implications. *Chemical Geology* 235, pp.262-275.

8 Appendix

Table A.1 : Grain size distribution, total nitrogen (TN), total carbon (TC), total organic carbon (TOC) as measured and total inorganic carbon (TIC) and TOC/TN ratio as calculated.

Sample	Depth (cm)	Sand (%)	Silt (%)	Clay (%)	Mean (Phi)	Skewness (Phi)	TN (%)	TC (%)	TOC (%)	TIC (%)	TOC%/TN(%)
07-SA-34 02	0,57-1,14	13,87	71,92	14,20	6,29	0,15	0,60	6,58	5,54	1,04	9,26
07-SA-34 04	1,71-2,28	10,01	71,03	18,95	6,76	-0,11	0,53	5,70	4,99	0,71	9,44
07-SA-34 06	2,85-3,42	6,19	73,56	20,26	7,38	-0,54	0,44	4,73	4,12	0,61	9,31
07-SA-34 08	3,99-4,56	18,45	70,51	11,07	5,89	0,46	0,33	3,40	2,78	0,62	8,48
07-SA-34 10	5,13-5,70	10,94	70,86	18,20	6,68	0,18	0,29	3,03	2,44	0,59	8,44
07-SA-34 12	6,27-6,84	20,68	64,53	14,84	6,19	0,33	0,27	2,74	2,26	0,48	8,40
07-SA-34 14	7,41-7,98	19,35	67,19	13,45	6,26	0,16	0,24	2,54	2,18	0,35	9,05
07-SA-34 16	8,55-9,12	23,64	64,15	12,21	5,97	0,25	0,24	2,53	2,20	0,33	9,22
07-SA-34 18	9,69-10,26	12,54	72,32	15,15	6,50	-0,05	0,23	2,55	2,25	0,30	9,86
07-SA-34 20	10,83-11,4	7,34	78,64	14,02	6,40	0,28	0,17	2,15	1,96	0,20	11,39
07-SA-34 22	11,97-12,54	13,60	72,58	13,81	6,24	0,18	0,18	2,42	2,25	0,17	12,50
07-SA-34 24	13,11-13,68	6,34	77,26	16,40	6,77	0,04	0,21	2,68	2,38	0,31	11,43
07-SA-34 26	14,25-14,82	11,15	75,41	13,43	6,46	0,07	0,25	2,74	2,41	0,34	9,65
07-SA-34 28	15,39-15,96	20,45	66,95	12,60	6,20	0,16	0,29	2,84	2,34	0,51	8,03
07-SA-34 30	16,53-17,1	22,54	65,31	12,12	5,99	0,14	0,27	2,84	2,42	0,43	9,00
07-SA-34 32	17,67-18,24	5,38	78,82	15,82	6,80	0,16	0,29	3,19	2,85	0,34	9,77
07-SA-34 34	18,81-19,38	22,05	66,22	11,77	5,92	0,18	0,31	3,62	3,25	0,37	10,32
07-SA-34 36	19,95-20,52	26,36	61,26	12,37	5,85	0,05	0,33	3,94	3,57	0,38	10,94
07-SA-34 38	21,09-21,66	9,89	75,37	14,75	6,44	0,15	0,26	3,60	3,41	0,20	12,93
07-SA-34 40	22,23-22,8	30,62	59,04	10,39	5,60	0,29	0,31	3,64	3,24	0,40	10,45
07-SA-34 42	23,37-23,94	15,65	70,82	13,53	6,32	0,13	0,31	3,68	3,43	0,26	11,01
07-SA-34 44	24,51-25,08	16,81	68,77	14,42	6,39	-0,12	0,37	4,22	3,84	0,39	10,44
07-SA-34 46	25,65-26,22	10,43	73,07	16,46	6,71	-0,07	0,46	5,09	4,69	0,40	10,11
07-SA-34 48	27,36-27,93	10,69	71,17	18,16	6,90	-0,27	0,48	5,26	4,71	0,54	9,89

8 Appendix

07-SA-34 50	28,5-29,07	4,61	75,88	19,50	7,20	-0,24	0,43	4,70	4,34	0,36	10,19
07-SA-34 52	29,64-30,21	18,12	66,83	15,05	6,43	-0,29	0,39	4,50	4,12	0,38	10,50
07-SA-34 54	30,78-31,35	6,75	74,51	18,77	7,09	-0,35	0,49	5,49	5,11	0,38	10,45
07-SA-34 56	31,92-32,49	12,55	74,40	13,05	6,25	0,21	0,49	5,42	4,93	0,49	10,10
07-SA-34 58	33,06-33,63	26,54	61,53	11,91	5,89	0,06	0,52	5,77	5,25	0,52	10,03

Table A.2: $\delta^{13}\text{C}$ and $\delta^{15}\text{N}$ isotope ratios

Sample	Depth (cm)	$\delta^{13}\text{C}$ (‰)	$\delta^{15}\text{N}$ (‰)
07-SA-34 02	0,57-1,14	-31,99	3,48
07-SA-34 04	1,71-2,28	-31,35	3,40
07-SA-34 06	2,85-3,42	-30,91	3,51
07-SA-34 08	3,99-4,56	-30,52	3,50
07-SA-34 10	5,13-5,70	-30,48	3,58
07-SA-34 12	6,27-6,84	-30,55	3,68
07-SA-34 14	7,41-7,98	-30,11	3,51
07-SA-34 16	8,55-9,12	-30,07	3,48
07-SA-34 18	9,69-10,26	-29,39	3,40
07-SA-34 20	10,83-11,4	-28,32	3,23
07-SA-34 22	11,97-12,54	-27,97	3,21
07-SA-34 24	13,11-13,68	-28,32	3,17
07-SA-34 26	14,25-14,82	-29,26	3,31
07-SA-34 28	15,39-15,96	-30,52	3,53
07-SA-34 30	16,53-17,1	-29,96	3,35
07-SA-34 32	17,67-18,24	-29,63	3,24
07-SA-34 34	18,81-19,38	-29,64	3,41
07-SA-34 36	19,95-20,52	-29,74	3,24
07-SA-34 38	21,09-21,66	-28,88	3,11
07-SA-34 40	22,23-22,8	-29,74	3,29

8 Appendix

07-SA-34 42	23,37-23,94	-29,85	3,14
07-SA-34 44	24,51-25,08	-30,47	3,02
07-SA-34 46	25,65-26,22	-30,99	2,96
07-SA-34 48	27,36-27,93	-31,25	3,05
07-SA-34 50	28,5-29,07	-30,67	3,01
07-SA-34 52	29,64-30,21	-30,35	3,02
07-SA-34 54	30,78-31,35	-30,60	2,90
07-SA-34 56	31,92-32,49	-30,62	2,79
07-SA-34 58	33,06-33,63	-30,01	2,57

Danksagung

Zuallererst möchte ich Prof. Dr. Ulrike Herzsuh für die Betreuung und die Unterstützung vor und während der Diplomarbeit und für das Heranföhren an die Palynologie danken. Ihre Anregungen und Hinweise, auch über den wissenschaftlichen Rahmen hinaus, haben mir oft geholfen.

Prof. Dr. Florian Jeltsch danke ich für seine Betreuung und Begutachtung dieser Arbeit und die lehrreichen Vorlesungen die mein Interesse an der Ökologie weiter gestärkt haben.

Bei dem ganzen Team des AWI Potsdam bedanke ich mich für ihre ausnahmslose Zuvorkommenheit und das stetige Vertrauen in mich und meine Fähigkeiten. Insbesondere möchte ich Ute Bastian für ihre Unterstützung und labortechnische Kompetenz, sowie allen Azubis, Hiwis, Diplomanden und Doktoranden für das tolle Arbeitsklima und die vielen schönen gemeinsamen Laborstunden, Kaffeepausen, Strickabende und Laufrunden vor, während und nach der Arbeit danken.

Hierbei gilt mein besonderer Dank Juliane Klemm, welche mir die Geheimnisse der Statistik näher brachte und immer ein offenes Ohr für palynologische und sonstige Fragen hatte. Michael Fritz danke ich für den Beistand bei unzähligen, arbeitsbezogenen Fragen und die moralische Unterstützung, sowie die gemeinsam verbrachten Zugfahrten und Gespräche beim Telegrafenberg erklimmen.

Boris Biskaborn, Dr. B. Dieckman und Gerald Müller danke ich für eine einmalige Expedition 2010!

Mein Dank gilt auch meinen Kommilitonen Katja und Laura für die schöne Studienzeit, wobei insbesondere Laura, mit ihrem Motivationsvermögen und ihrer Ausdauer ein ganz liebes Dankeschön für die vielen gemeinsam verbrachten Stunden und ihre Unterstützung in allen Lebenslagen gebührt.

Für das bereitwillige Korrekturlesen und die fachmännische Unterstützung in PC-Fragen danke ich ganz lieb Andrè, Nele und Stephan.

Ganz besonders danke ich meiner Familie für das Ermöglichen des Studiums, sowie ihre durchgängige Unterstützung, in seelischer moralischer, aber auch finanzieller Hinsicht. Meiner Mom möchte ich zudem für ihr unerschöpfliches Wissen und ihre Ratschläge in allen Lebenslagen danken.

Ein ganz lieber Dank gebührt insbesondere meiner kleinen Familie, meinen zwei Sonnenscheinen, dafür, dass sie mir immer wieder zeigen was wirklich wichtig ist. Dabei danke ich meinem Freund Udo, dem Fels in meinem etwas chaotischen Leben, für seinen Beistand, Rückhalt und Glaube an mich.

Abschließend möchte ich mich allen, Freunden, Kollegen und Bekannten, bedanken, die zum Gelingen dieser Arbeit beigetragen und mich während des Studiums unterstützt haben.

Selbstständigkeitserklärung

Hiermit versichere ich, dass ich die vorliegende Arbeit selbstständig verfasst und keine anderen als die angegebenen Quellen und Hilfsmittel verwendet habe. Alle von Autoren wörtlich übernommenen Stellen, wie auch sich an die Gedanken anderer Autoren eng anlehrende Ausführungen meiner Arbeit, sind unter Angabe der Quelle kenntlich gemacht.

Potsdam 08.09.2010

Liv Heinecke